TRIUMF

ANNUAL REPORT
SCIENTIFIC ACTIVITIES
2002

ISSN 1492-417X

**CANADA'S NATIONAL LABORATORY
FOR PARTICLE AND NUCLEAR PHYSICS**

OPERATED AS A JOINT VENTURE

MEMBERS:

THE UNIVERSITY OF ALBERTA
THE UNIVERSITY OF BRITISH COLUMBIA
CARLETON UNIVERSITY
SIMON FRASER UNIVERSITY
THE UNIVERSITY OF VICTORIA

ASSOCIATE MEMBERS:

THE UNIVERSITY OF MANITOBA
McMASTER UNIVERSITY
L'UNIVERSITÉ DE MONTRÉAL
QUEEN'S UNIVERSITY
THE UNIVERSITY OF REGINA
THE UNIVERSITY OF TORONTO

UNDER A CONTRIBUTION FROM THE
NATIONAL RESEARCH COUNCIL OF CANADA

DECEMBER 2003

The contributions on individual experiments in this report are outlines intended to demonstrate the extent of scientific activity at TRIUMF during the past year. The outlines are not publications and often contain preliminary results not intended, or not yet ready, for publication. Material from these reports should not be reproduced or quoted without permission from the authors.

Experiment 614
TWIST – the TRIUMF weak interaction symmetry test
(G.M. Marshall, TRIUMF)

TWIST is an experiment to measure precisely the parameters describing the energy and angular dependence of positrons (e^+) emitted from the decay of polarized positive muons (μ^+). It uses the M13 beam line to provide a high luminosity beam of highly polarized surface muons, produced by pions decaying at rest near the surface of the 1AT1 pion production target. The muons are guided axially into a large, uniform, 2 T solenoidal magnetic field where they stop in a thin planar target at the centre of a precisely constructed, low-mass array of drift chambers (Fig. 1). The polarization of the muon beam, $\vec{\mathcal{P}}_\mu$, is preserved to a high and predictable degree in the process. When the muons decay with a mean lifetime of 2.2 μs, the array of chambers records the tracks of the e^+ in the magnetic field, allowing the measurement of e^+ momentum for several thousand decays every second.

Such a large number of events means that the characteristics of the decay (e^+ energy and angular distributions) can be measured with unprecedented accuracy, and that the many possible sources of systematic uncertainties can be investigated efficiently. The distributions are described by four parameters (ρ, η, δ, and ξ), widely referred to as the Michel parameters. The distributions, and thus the values of the four parameters, are exactly predicted by the standard model. The goal of TWIST is to search for deviations from the predictions and thus to subject the model to very stringent tests, by measuring ρ, δ and $\mathcal{P}_\mu\xi$ to a few parts in 10^4.

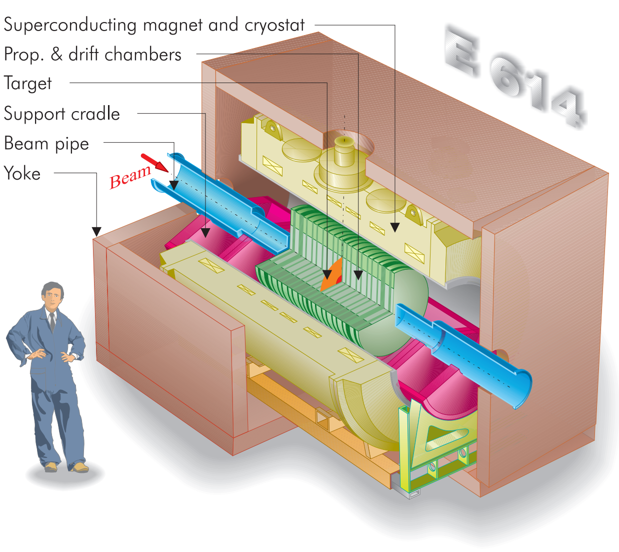

Fig. 1. The TWIST spectrometer.

This represents an improvement of more than one order of magnitude over the existing precision. An additional advantage is that the values are derived simultaneously and consistently from the same data set, thereby strengthening the outcome with respect to correlated uncertainties in the different parameters.

While the standard model has been very successful so far at predicting diverse phenomena in the interactions of subatomic particles, it is widely regarded as an approximation to a more fundamental theory, one which may be more symmetric in left-right handedness and in particle-antiparticle character. TWIST may be able to elucidate some of the qualities of the more fundamental theory.

Progress towards the goals of TWIST

Following the first operation of most of the spectrometer's components in beam during an engineering run in the fall of 2001, the TWIST experiment made significant progress in 2002, thanks to the support and assistance of many individuals at TRIUMF.

Solenoid

The solenoid magnetic field was mapped, using an array of Hall probes and a data acquisition system which automatically measured and recorded the longitudinal field components while the array was rotated and translated throughout the positron tracking volume. The probes were calibrated *in situ* with an NMR device, and a partial survey was also made using NMR to check for consistency and precision. The results were compared with predictions of the OPERA simulation program. Parameters were adjusted in OPERA by comparing with the measurements, enabling OPERA to provide a field map of the tracking volume which is in good agreement with the survey. This map is now used by the GEANT simulation of particles in the detector, and is being incorporated into the tracking and analysis software.

While ramping the field of the superconducting solenoid near its operating point in preparation for the first physics runs, the solenoid quenched. The resulting loss of cryogens (liquid helium and nitrogen), coupled with a previously identified small leak in the solenoid vacuum vessel, precipitated a nearly complete warmup of the cryogenic system of the superconductor. Subsequent cooling took much longer than anticipated, but the solenoid was again ready for operation in August. Fortunately, no damage to the solenoid or the detector system occurred from the quench.

Detector

There were only a few very minor problems encountered in the engineering run in 2001. One broken wire (of 4608) and three oscillating planes (of 56) were quickly and completely repaired. The high quality and precision of construction of the chambers and their gas systems have led to a very reliable, robust detector assembly. The chambers demonstrated full efficiency (>99.9%) and experienced no high voltage trips during normal operation throughout six months of beam time in 2002.

Data acquisition

The on-line data acquisition was expanded and improved. The system is now capable of recording data at the high rates required (event rate 5000 s^{-1}, event size 1.5 kB, data rate 8 MB s^{-1}), and upgrades to this can be included if necessary. This is made possible in part by a new high-capacity tape system (SDLT 320 standard) which additionally reduces the cost of the recording medium by a significant amount. Precise periodic monitoring takes place for many parameters which can affect data quality, such as temperatures, pressures, voltages, currents, magnetic fields, primary and secondary beam parameters, etc. The values recorded are used not only during data analysis, but also to create alarms for conditions out of specification which signal problems that must be corrected by the experimenter. On-line documentation describing responses to most problems has been provided. Some of the periodically measured values, the NMR magnetic field measurements in the dipoles of M13, are now used to automatically control the fields within very tight tolerances by communication with the recently developed EPICS control system for M13.

Software and analysis

Throughout the year, taking advantage of data obtained in the engineering run as well as the physics runs, the software used in simulation and analysis was dramatically improved. The GEANT3 simulation was further customized by extending and including processes which are expected to be important for TWIST physics measurements. A procedure was established for testing and adjusting the alignment of the planar drift chambers in the analysis software. Another procedure for calibration of the times of drift chamber hits on a wire-by-wire basis was developed and applied. The helix fitting procedures used in the analysis code were tested on both simulated and real data, improving the precision of track reconstruction.

A procedure has been defined by which the data can be analyzed in a way which is blind to the final results, in order to avoid possible human biases. The principle has been used by many other collaborations, but the nature of the TWIST analysis requires some special techniques by which the data are fit to a sum of simulated spectra generated with hidden Michel parameters which are different from the accepted values. When the fits are completed and satisfactory, the hidden values are revealed and the results of the fit are used to calculate the true experimental values for the Michel parameters.

In order to be able to process the large amount of data and to match it with a comparable number of simulated events, a small analysis cluster consisting of fifteen dual-CPU nodes (AMD 1.8 GHz processors) and a tape library device were purchased with an NSERC equipment grant. Although still inadequate for our full requirements, the analysis and simulation rates were greatly improved.

First measurements

Data were taken in the fall of 2002, with the goal of determining two of the Michel parameters, ρ and δ, with a precision of better that one part in 10^3. While this level of statistical precision can be reached using only a few days of beam (a data set of some 10^8 events is adequate), the investigation of possible systematic uncertainties takes much longer. Altogether, approximately 6×10^9 events were recorded, comprising many separate measurements of the Michel parameters under different experimental conditions, in order to measure quantitatively the effects of the changes. Data sets were obtained corresponding to such variables as different detector efficiencies, solenoidal fields, muon beam characteristics (polarization, stopping position, focus position), trigger rates, and backscattered event rates. Figures 2 and 3 show the momentum and angular distributions, respectively, from one data set.

A critical task for TWIST is to test and validate both the analysis software and simulation programs. With the availability of the first data, this has begun. Agreement between the simulated and measured muon stopping distributions is impressive. Although there is no truly monochromatic positron calibration source

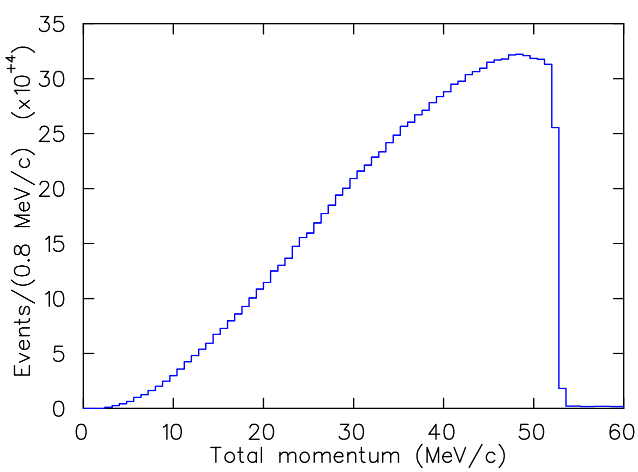

Fig. 2. Momentum distribution from one data set; events in the range of about 15 to 50 MeV/c are considered to be within the fiducial volume.

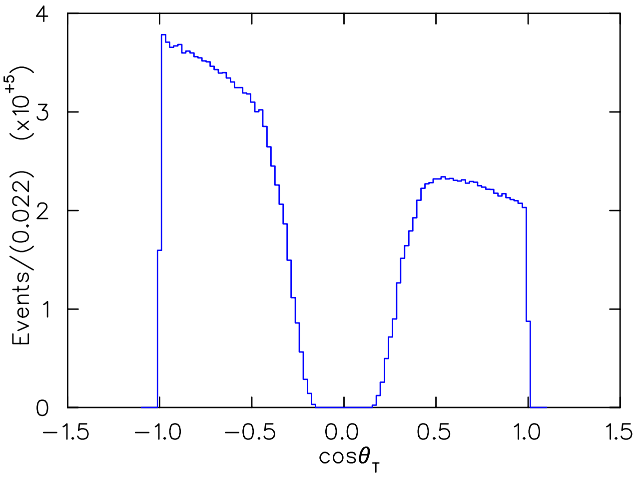

Fig. 3. Angular distribution from one data set; events in the range of about $0.5 < |\cos\theta_T| < 0.95$ are considered to be within the fiducial volume, while the region near $\cos\theta_T = 0$ is not within the spectrometer acceptance.

which can populate the spectrometer angular acceptance, the symmetry of the detector allows one half to be used to independently define a positron track to the limits of the detector precision, while the other half can be used to analyze another part of the same track. This is accomplished by using muons which have been selected to stop not in the target at the centre of the detector, but near either end of the detector. Comparison of the two halves permits checking characteristics such as pattern recognition, reconstruction efficiency, and resolution in angle and momentum. Moreover, comparisons can also be made using the simulation under the same conditions, to help to validate the physics of simulated positron motion through the detector.

Next steps

The analysis of the data taken in 2002 is proceeding at the limits of the human and computing resources of the group. It is expected that this analysis will be completed in 2003. Meanwhile, improvements to the muon beam and to its characterization, using a newly constructed low-density time expansion chamber, will enable TWIST to proceed with the measurement of $\mathcal{P}_\mu\xi$ to a precision of one part in 10^3. With the experience gained in the process, the challenges of the measurements to the ultimate statistical and systematic capabilities of the spectrometer can be met.

ATLAS Experiment at the LHC

(C. Oram, TRIUMF)

As described in detail in the 1996 Annual Report, ATLAS is building a general purpose *pp* detector which is designed to exploit the full discovery potential of the Large Hadron Collider (LHC) at CERN. The TRIUMF group is responsible for the management and engineering of the hadronic endcap (HEC) calorimeter, and the feedthroughs for the endcap cryostat. For the HEC, this year has seen the completion of module production and the assembly of the two wheels of the first endcap. The wheel assembly at CERN is led by a TRIUMF staff member.

Physics goals

The present theoretical understanding of elementary particles is in the context of the standard model. It is a remarkably successful model, providing predictions which have been consistently confirmed by experiments for over two decades. Its agreement with experimental results, to enormous accuracy in some cases, makes it the most accurately verified model in science. Of the many elementary particles contained in the standard model, only the Higgs remains to be discovered. The central goal of ATLAS is the search for the Higgs particle.

There are good theoretical reasons to believe that the discovery of the Higgs will at least contain hints at, and more likely direct evidence of, what lies beyond the standard model. If the Higgs is composite, its existence requires as yet unknown ultra-strong forces. If it is elementary, it would be the only spinless particle to be discovered so far. There is a theoretical “naturalness” problem for the masses of spinless particles. In the standard model, which is a highly nonlinear dynamical system, the elementary particles tend to take on the heaviest of all possible mass scales which in such a model are at inaccessible energies and inconsistent with other requirements of the model. All other particles discovered thus far have natural mechanisms, such as gauge and chiral symmetries, for protecting their masses so that they can lie in the observable range. For the Higgs particle, there is no such symmetry in the present model. The only theoretical scenarios which leave the Higgs particle light enough to observe are hypothetical ones, either technicolour or supersymmetry, both radical departures from the present structure of the standard model. If the Higgs is seen at the LHC, one of these scenarios should be seen at the same time.

Particle theory has progressed enormously over the last few decades with many appealing scenarios for physics beyond the standard model. The most likely of these is supersymmetry and the boldest of these is superstring theory. These theories are intimately related and are both radical ideas which promise a new conceptual framework for understanding elementary particles. Though far from being complete theories so far, there are superstring models which resemble the standard model in their low energy limit. These models have a great appeal as they contain a unification of fundamental forces which includes gravity. They have already had substantial impact on gravitational physics where, for example, in addition to the long sought reconciliation of gravity with quantum mechanics, they have been used to derive a fundamental understanding of black hole thermodynamics. Superstring theory is still in its infancy, but progress has been dramatic and the promise of great things to come has captured the imagination of a substantial fraction of the world's theoretical particle physicists.

The present theoretical view is that the conventional grand unification of the strong, weak and electromagnetic forces can only work in the supersymmetric extension of the standard model. In that model, the grand unified energy scale is only two decades below the Planck scale, the ultimate energy where spacetime itself has quantum fluctuations. It is not out of the realm of imagination that, at energy scales where supersymmetry would be observed, evidence for an ultimate theory of everything, at least everything that can exist once spacetime is formed, is within human grasp.

Experiments at the LHC, where the ATLAS detector will take data, will probe the energy region where the Higgs particle, possibly supersymmetry, or other structures will be visible. This will be the first experimental probe of an energy region where fundamentally new physics is expected to occur in many years. There is every reason to believe that the results will be among the most dramatic ever.

Basic ATLAS design considerations

The most prominent issue for the LHC is the quest for the origin of the spontaneous symmetry-breaking mechanism in the electroweak sector of the standard model (SM). This is related to one of the most fundamental questions of physics: What is the origin of the different particle masses? New direct experimental insight is required to answer this question.

One of the possible manifestations of the spontaneous symmetry-breaking mechanism could be the existence of a SM Higgs boson (H), or of a family of Higgs particles ($H^{\pm}$, h, H and A) when considering the minimal supersymmetric extension of the standard model (MSSM). The Higgs search is therefore used as a first benchmark for the detector optimization. For the SM Higgs, the detector has to be sensitive to the following processes ($\ell = e$ or μ) in order to cover the full mass range above the discovery limit set by the final LEP operation in the fall of 2000:

$H \to b\bar{b}$ from WH, ZH and $t\bar{t}H$ using a $\ell^{\pm}$ and b-tagging,
mass range $80 < m_H < 100$ GeV;

$H \to \gamma\gamma$
mass range $90 < m_H < 150$ GeV;

$H \to WW^* \to \ell^{\pm}\nu\ell^{\pm}\nu$
mass range $150 < m_H < 200$ GeV;

$H \to ZZ^* \to 4\ell^{\pm}$
mass range 130 GeV $< m_H < 2m_Z$;

$H \to ZZ \to 4\ell^{\pm}, 2l^{\pm} + 2\nu$
mass range $m_H > 2m_Z$;

$H \to WW, ZZ \to l^{\pm}\nu + 2$ jets, $2\ell^{\pm} + 2$ jets from WW, ZZ fusion using tagging of forward jets for m_H up to about 1 TeV.

In addition to signatures similar to these, the MSSM Higgs searches also require sensitivity to processes such as:

$$\begin{aligned} A &\to \tau^+\tau^- \quad \to e\mu + \nu\text{'s} \\ &\qquad\qquad \to \ell^{\pm} + \text{hadrons} + \nu\text{'s}; \\ H^{\pm} &\to \tau^{\pm}\nu \quad \text{from } t\bar{t} \to H^{\pm}W^{\mp}b\bar{b} \text{ and using} \\ &\qquad\qquad \ell^{\pm} \text{ tag and } b\text{-tagging} \\ &\to 2 \text{ jets}\,. \end{aligned}$$

The observable cross sections for most of these processes are small over a large part of the mass range to be explored at the LHC. Hence it is important to operate at high luminosity, and to maximize the detectable rates above backgrounds by high-resolution measurements of electrons, photons, and muons.

Canada's participation in ATLAS

The Canadian group consists of about 35 grant eligible physicists from TRIUMF, University of Alberta, Carleton University, Simon Fraser University, University of British Columbia, Université de Montréal, University of Toronto, University of Victoria, and York University. We are strongly involved in three construction projects centred around detecting hadrons in the endcap region: the hadronic endcap project, the hadronic portion of the forward calorimeter project, and the pipeline electronics for calorimetry. In addition, we are committed as part of our common project contribution to providing the feedthroughs for the two endcap cryostats. TRIUMF is directly involved in all of these projects, and in the trigger and physics simulations.

The hadronic endcap project

The hadronic endcap (HEC) calorimeter is a liquid argon sampling calorimeter with copper absorbers [ATLAS Collab., ATLAS Liquid Argon Technical Design Report, December 15 (1996)]. A concise overview of this design was provided in the 1996 TRIUMF Annual Report. An artist's impression of a module can be seen in Fig. 4. In each endcap cryostat sit four detector systems: nearest the interaction region is the presampler, followed by the electromagnetic endcap (EMEC) and the HEC. At the inner diameter around the beam pipe is the forward calorimeter (FCAL).

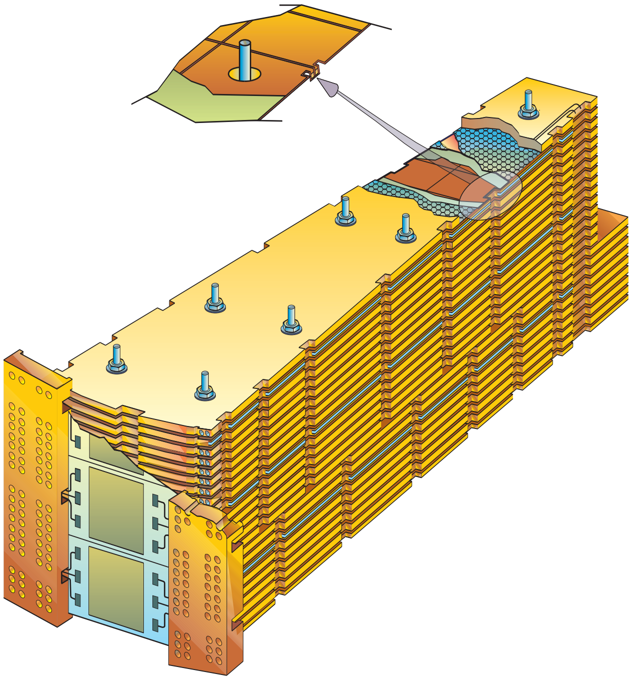

Fig. 4. Artist's impression of a hadronic endcap module.

Hadronic endcap module production

By the middle of the year the TRIUMF group was 100% complete on module production, and by September had shipped all major components. The copper machining facility at the University of Alberta completed all machining for the European groups early in 2002. Hence by year end, production at TRIUMF was limited to making dust covers for the completed wheels at CERN.

Test beam measurements of the hadronic endcap modules

This year saw the publication [Dowler *et al.*, Nucl. Instrum. Methods **A482**, 94 (2002)] of the extensive set of standalone beam tests of the hadronic endcap. This finished our quality control criteria in which we measured 1/8th of our series module production in the test beam at CERN. All the series modules are cold tested. By the end of 2002 we had tested 120 of the 132 modules that constitute the two HEC endcaps in ATLAS.

A test beam period in the summer on the CERN H6 beam line has successfully tested the combined performance of the HEC and EMEC series production modules of the endcap calorimeter system. The H6 beam line provides beams from 20 to 180 GeV. Initial analysis of the data shows the data is of good quality, and the response is within the design goals. This is an important milestone for the group as these measurements form the basis of the calibration of the system as it will be used at LHC beam startup.

To be ready for ATLAS, a further test beam measurement with the calorimeters near the beam line is required. This test will use standard EMEC and FCAL modules, along with purpose built small "inner radius" HEC modules. During 2003 these small inner radius HEC modules will be constructed.

Wheel assembly at CERN

32 modules of the HEC form a wheel. There are two wheels at each end of ATLAS, so we must construct 128 modules into four wheels. The equipment to undertake this is a Canadian responsibility. These four wheels and the two wheels of the EM calorimeter, which go in the same cryostat, are assembled in the horizontal orientation. Hence each wheel, which weighs about 90 tonnes, must be taken from its assembly table, rotated to the vertical and moved to the cryostat. This rotation and translation of equipment is a Canadian responsibility. The engineering was undertaken by a collaboration between Alberta and TRIUMF personnel. The production of the equipment was by Canadian industry. This equipment was delivered to CERN in January, 2002. It was successfully assembled and tested, both for mechanical loading and operation with other systems. Two wheels were constructed this summer, both on schedule. Both wheels have been rotated from the horizontal into the vertical. The rotated wheels have successfully passed all their extensive electrical tests, and are well within their allotted envelopes. The sag of the rotated wheel was measured to be 0.3 mm, which is in agreement with prior calculations. Figures 5 and 6 show respectively the first and second wheel being rotated. Wheel assembly will be completed in early 2004.

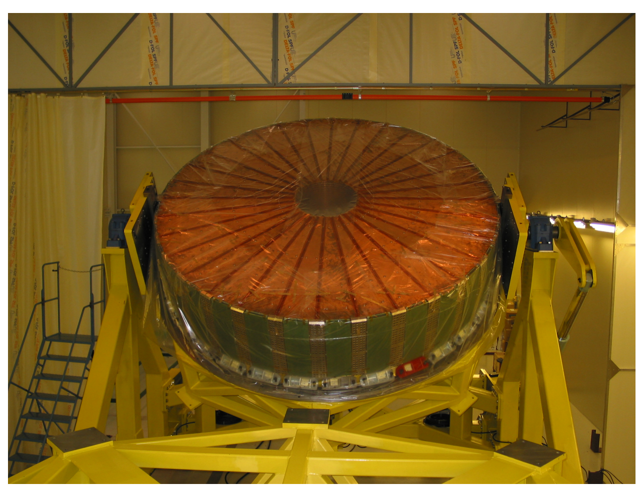

Fig. 5. First front HEC wheel being rotated.

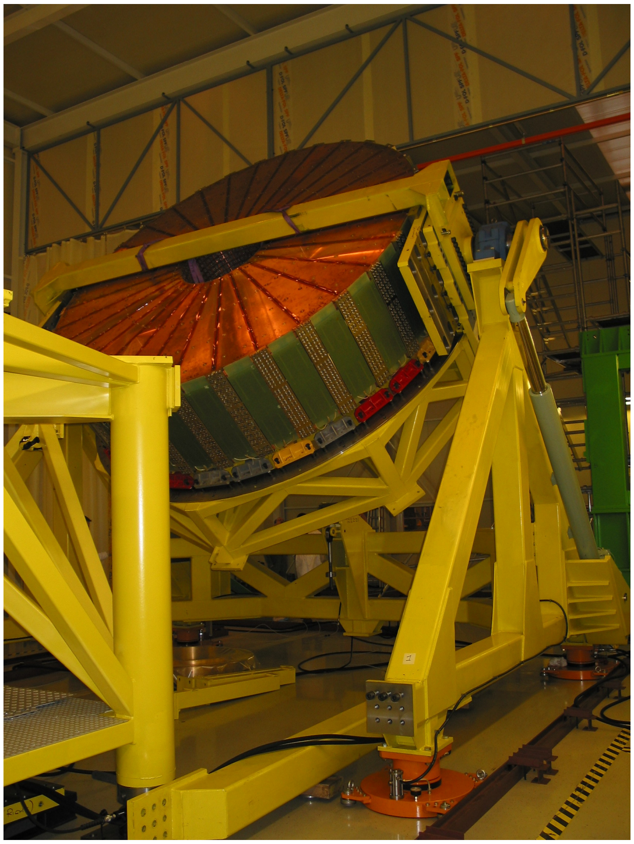

Fig. 6. First rear HEC wheel being rotated.

The ATLAS endcap signal feedthroughs

(M. Lefebvre, Victoria)

The TRIUMF group is responsible for the engineering of the HEC and contributes to the production of high density cryogenic signal feedthroughs for both endcap cryostats. The feedthroughs are critical to the success of ATLAS. They have been built and tested at the University of Victoria by TRIUMF and Victoria staff. The endcap signal feedthroughs are currently (December, 2002) being installed on one of the two endcap cryostats. The operation is expected to last until the end of February, 2003. The second installation period is scheduled for early summer, 2003. The ATLAS endcap signal feedthrough project was covered in detail in the 2001 Annual Report. This report focuses on recent progress.

Reviews

A Canadian involvement in the endcap signal feedthroughs was already proposed in 1995. From the \$12.2 M Major Installation Grant awarded to ATLAS in the 1997–98 competition, a total of \$4.28 M is earmarked for the endcap signal feedthrough project. The most recent status report was presented at the last NSERC ATLAS Review, held at TRIUMF December 5–7, 2002.

Overview of the project

The ATLAS liquid argon calorimetry is composed of a barrel section and two endcap sections. Each endcap cryostat contains an electromagnetic calorimeter, two wheels of one HEC, and a forward calorimeter. The calorimeter signal and calibration lines are routed to the outside of each endcap cryostat via 25 feedthrough assemblies arranged approximately equally spaced in azimuth. The low voltage needed to operate the endcap hadronic calorimeter preamplifiers, which are located in the cold, are also supplied via the signal feedthroughs as well as various monitoring lines.

The design is based on gold plated conductive pins insulated and sealed by glass inserts in a stainless steel carrier. The carriers are then welded into the cold and ambient (temperature) flanges. A total of 1920 signal and calibration lines per feedthrough assembly is required in the chosen design. The ambient and cold flanges are connected by a bellows to isolate the feedthrough vacuum from the cryostat inter-vessel vacuum. The cold flange is attached to a transition piece, known as a funnel, which is welded to the cryostat via a bi-metallic joint. The electrical signals are brought from the calorimeter to the cold flange by coaxial kapton cables; these are called pigtail cables. Cables located in the vacuum between the cold and the ambient flange, i.e. inside the bellows, carry the signals through the cryostat wall; these are called vacuum cables. For each endcap, four feedthrough assemblies also carry the low voltage for the HEC preamplifiers. Figure 7 shows an overview drawing of one endcap signal feedthrough.

Procurement of components

Pigtail cables

The development of the pigtail cables was part of a larger effort to develop signal and calibration cables for the whole of the liquid argon (LAr) readout chain. They were purchased through Orsay, along with the other ATLAS LAr cables, from Axon. A Memorandum of Understanding for the procurement of the endcap pigtail cables was signed by Orsay and ATLAS-Canada. A detailed procurement schedule was developed, and reception of pigtails in Victoria was completed in the fall of 2002.

Pin carriers

Extensive and detailed tests comparing the ceramic and glass pin carrier technologies were made in 1997 and 1998. Both technologies were found suitable for our project. The green light was given at the feedthrough Production Readiness Review (held in CERN on January 29, 1999) to purchase glass technology pin carriers made of low inclusion 304 L stainless steel. The order was placed in June, 1999. Reception was completed early in 2002.

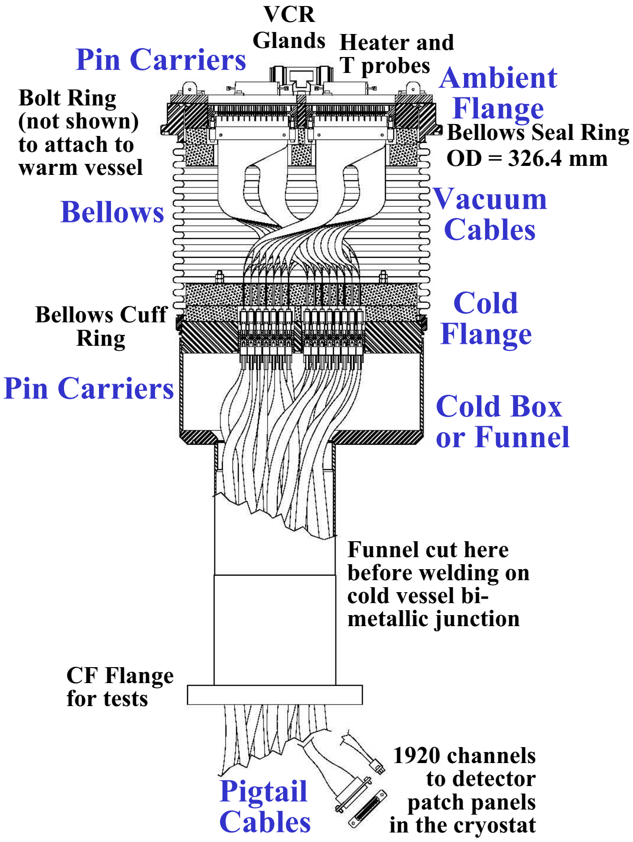

Fig. 7. Overview drawing of one endcap signal feedthrough, identifying its most important components.

Assembly and installation

A total of 50 feedthrough assemblies plus 5 spares have been produced (see Fig. 8) following a detailed assembly procedure, quality plan and quality assurance plan. These include the description of the testing of components from their arrival in Victoria through the completion of feedthrough units. Complete material traceability is ensured through the use of detailed traveller sheets. The funnel and cold flange of each feedthrough assembly are part of the cryostat pressure vessel. An officially licensed company has done the welding and extensive testing to conform to accepted welding code.

The shipment of feedthrough assemblies to CERN is done by air freight. All but five assemblies are now in CERN. Upon arrival at CERN, each feedthrough assembly is subjected to an ambient temperature leak test and a basic electrical test. We are responsible for these tests. The required testing equipment was commissioned at CERN in October, 2001, when the first feedthrough assemblies arrived at CERN.

The installation of the feedthrough assemblies on the cryostat is a delicate and complex operation. Although the feedthrough installation is not a Canadian responsibility, our group is actively assisting during the

Fig. 8. Vacuum cables being installed on a feedthrough by Paul Birney (TRIUMF) at the University of Victoria.

operation. In particular, given the softness of the pins, members of our team will manually connect the so-called warm cables that join the outside of the ambient flange to the electronics crate baseplane. Each feedthrough assembly, once welded on the cryostat, must also be electrically tested.

The installation of the feedthrough assemblies on the first endcap cryostat (see Fig. 9) started on December 2, 2002 and is expected to last until the end of February, 2003. As of December 20, 2002, six feedthrough assemblies have been successfully installed (see Fig. 10). Installation on the second cryostat is scheduled for early summer, 2003. It is expected that Canada's involvement in the feedthrough project will end during 2003 with the connection of the warm cables to the ambient flange.

Fig. 9. The first endcap cryostat of the ATLAS liquid argon calorimeter after arrival at CERN, still in its transport cradle (April, 2002).

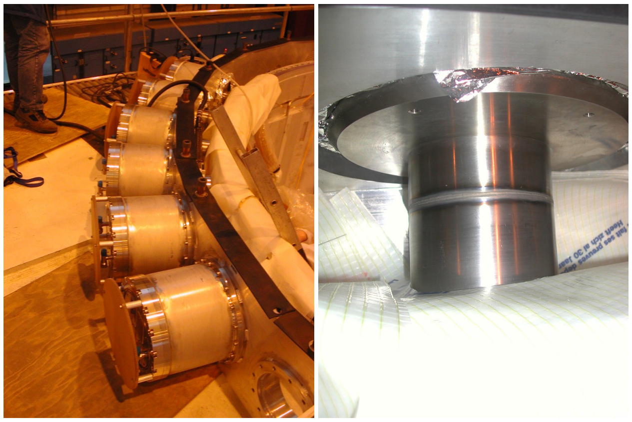

Fig. 10. First six feedthrough units installed on the first endcap cryostat (December, 2002) and a close-up of one of the welds. Photos by Aboud Falou, Orsay.

Canadian participants in ATLAS

Investigators: J. McDonald, J. Pinfold, M. Vincter (Alberta); D. Gingrich, P.W. Green (Alberta/TRIUMF); J. Armitage, M. Dixit, G. Oakham (Carleton); P. Depommier, C. Leroy, J.-P. Martin (Montréal); G. Azuelos (Montréal/TRIUMF); G. Couture (Montréal/UQAM); M.C. Vetterli (SFU/TRIUMF); D.C. Bailey, R.S. Orr, P. Sinervo, W. Trischuk (Toronto); P. Krieger, J.F. Martin (Toronto/IPP); M. Losty, C. Oram (TRIUMF); D. Axen (UBC); A. Astbury, R. Keeler, M. Lefebvre (Victoria); R. McPherson, R. Sobie (Victoria/IPP); S. Bhadra (York).

Collaborators: S. Liu, R. Soluk, S. Wheeler (Alberta); B. Caron (Alberta/TRIUMF); M. Khahkzad (Carleton); R. Mehdiyev (Montréal); Kyung Kwang Joo (Toronto); S. Chekulaev, H. Stenzel, M. Wielers (TRIUMF); M. Fincke-Keeler, N. Kanaya (Victoria).

Graduate students: N. Buchanan, L. Chen, C. Cojoocaru, B. Dowler, J. de Jong, R. McDonald, Wei-Yuan Ting (Alberta); G. Belanger, B. Williams (Carleton); P.H. Beauchemin, G. Fubiani, M.H. Genest, C. Lebel, R. Mazini, F. Marullo, P. Roy (Montréal); K. Martens (Toronto); M. Dobbs, T. Ince, V. Singh (Victoria).

BaBar Experiment at the Stanford Linear Accelerator Center

(C. Hearty, UBC)

Introduction

BaBar is an experiment to study the electroweak sector of particle physics using B mesons produced at the high-luminosity e^+e^- collider PEP-II. The primary physics goal is to observe and quantify CP violation in B mesons, but more generally, it is to test the standard model description of electroweak physics and to look for new physics beyond the standard model. The charged weak force is described by the CKM matrix in the standard model, and the central physics goals of BaBar are often described in terms of overconstraining the "unitarity triangle", a geometrical representation of the CKM matrix. BaBar's measurement in 2001 of the angle β of this triangle established that CP is violated in B decay.

The BaBar detector was designed, constructed and assembled prior to the start of the first data run in October, 1999. The drift chamber, one of six major detector systems, was constructed at TRIUMF.

Activities of the collaboration

BaBar collected data for seven months in 2002. The remaining five months constituted a major shut down, during which all components interior to the drift chamber (the support tube, silicon vertex tracker, beam pipe, and the final focus dipole and quadruple magnets) were removed. The primary purpose was to install additional cooling to allow beam currents above the design value. This seems to have been successful: as of early 2003, luminosity was approximately 30% above design. A small number of failed vertex tracker components were fixed as well.

An unfortunate accident during the removal of the support tube damaged the beryllium inner cylinder of the drift chamber, producing a crack approximately 10 cm in length. Although there was no loss of structural integrity, the chamber was unable to hold pressure. The crack was patched during the shutdown and subsequent measurements indicate that repairs are fully gas tight.

BaBar has made good progress in studying a second angle α of the unitarity triangle using the decay $B^0 \to \pi^+\pi^-$. Although higher-order diagrams make the extraction of α difficult, an initial step would be the observation of CP violation in this final state. BaBar, as of yet, does not see a significant asymmetry (Fig. 11). This is in contrast to Belle, which sees maximal asymmetry in this channel.

Activities of the local group

The local group continues to study charmonium ($c\bar{c}$) mesons. A paper describing the inclusive production of charmonium mesons in B decays was accepted for publication by Physical Review D. Branching fractions were measured for the inclusive production of the J/ψ, $\psi(2S)$, χ_{c1}, and χ_{c2}. The branching fractions were also presented as a function of the centre-of-mass momentum p^* of the mesons and of the helicity of the J/ψ.

The p^* distribution of the J/ψ (Fig. 12) is especially interesting. Compared to a recent non-relativistic QCD calculation, there is a significant excess at low momentum. Possible sources of the excess include an

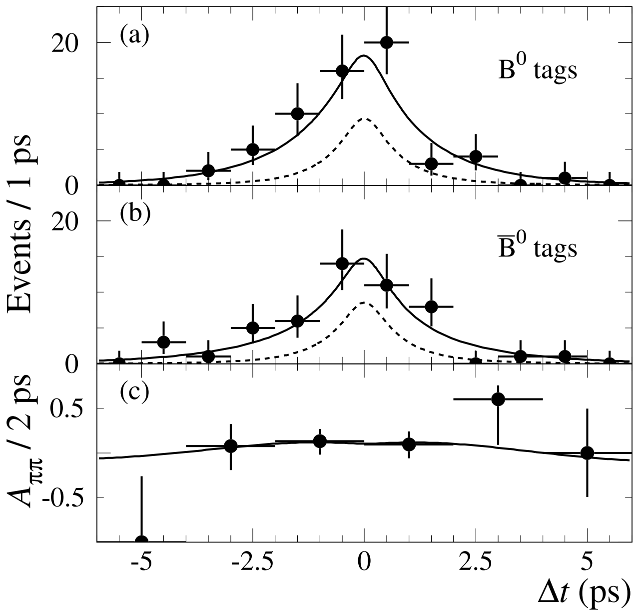

Fig. 11. Number of CP ($\pi^+\pi^-$) final state candidates (a) with a B^0 tag N_{B^0} and (b) with a $\bar{B}^0$ tag $N_{\bar{B}^0}$, and (c) the raw asymmetry $(N_{B^0} - N_{\bar{B}^0})/(N_{B^0} + N_{\bar{B}^0})$, as functions of the time difference between the signal and tag decay.

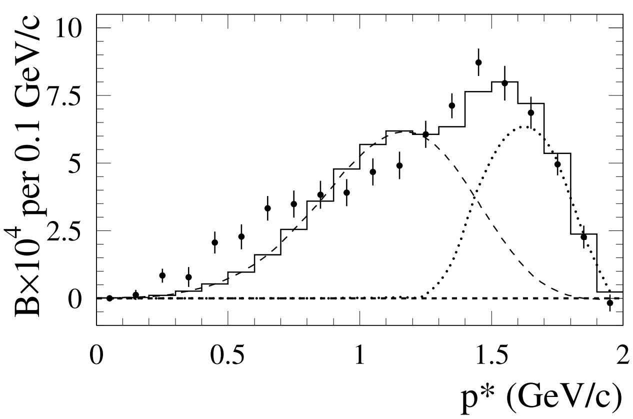

Fig. 12. Centre-of-mass momentum of J/ψ mesons produced directly in B decays (points). The histogram is the sum of the colour-octet component from a recent NRQCD calculation (dashed line) and the colour-singlet $J/\psi K^{(*)}$ component from simulation (dotted line).

intrinsic charm component of the B or the production of an $s\bar{d}g$ hybrid in conjunction with a J/ψ. Another possibility is that the excess is from decays of the form $B \to J/\psi$ baryon anti-baryon. The rate of this type of decay could be enhanced by the intermediate production of exotic states allowed by QCD but not yet observed, including nuclear-bound quarkonium (a $c\bar{c}$ pair bound to a nucleus) or baryonium, a baryon-antibaryon bound state.

These possibilities are being pursued in current analyses.

BNL E787/949/KOPIO
Measurement of $K \to \pi\nu\bar{\nu}$ and other rare decays

(D. Bryman, UBC)

Among possible measurements relating to CP violation, four "golden" processes which stand out as theoretically unambiguous will allow complete elucidation of CP violation in the standard model (SM). Two are the asymmetries in $B \to \Psi K_s$ decays, and the ratio of B_s to B_d mixing. The others are the branching ratios of the charged and neutral $K \to \pi\nu\bar{\nu}$ decays. These rare kaon decays offer unique opportunities to scrutinize higher order phenomena associated with quark mixing and charge-parity (CP) non-invariance.

In the SM, using current data on m_t, m_c, V_{cb}, $|V_{ub}/V_{cb}|$, ϵ_K, $\bar{B}-B$ mixing, etc., the branching ratio of $K^+ \to \pi^+\nu\bar{\nu}$ is expected to be $B_+ = 7.5 \pm 2.9 \times 10^{-10}$. SM expectations for the branching ratio of $K_L^0 \to \pi^0\nu\bar{\nu}$ are at the level $B_0 = 3 \times 10^{-11}$.

E787/949

The decay $K^+ \to \pi^+\nu\bar{\nu}$ has been the object of E787 and its sequel E949 at the Alternating Gradient Synchrotron (AGS) at Brookhaven National Laboratory (BNL). Initial data from E787 yielded the first evidence for the $K^+ \to \pi^+\nu\bar{\nu}$ decay. This year the final result from E787 was published [Adler *et al.*, Phys. Rev. Lett. **88**, 041803 (2002)] based on the full data set which doubled the previously reported sensitivity. Two events of the ultra-rare $K^+ \to \pi^+\nu\bar{\nu}$ decay have now been observed and the branching ratio remains consistent with the SM expectation.

Substantial upgrades to the E787 detector system have been made during the past two years in preparation for E949 aimed at reaching a sensitivity of $(8-14) \times 10^{-12}$, roughly an order of magnitude below the SM prediction. Since E949 will be the primary (or only) AGS user, the proton beam on target is intended to have an effective luminosity improvement of 56% over previous running conditions while keeping instantaneous rates at the same level. E949 running with higher instantaneous rates will also be attempted to increase the sensitivity.

In E949, a 700 MeV/c positive kaon beam with a K/π ratio of 4:1 passes through a series of active elements and passive degrader materials to be stopped in a scintillating fibre target at the centre of the detector. The TRIUMF group constructed a new set of more highly segmented beam counters designed to achieve improved spatial resolution at the hodoscope where the incoming particles enter the target. In order to improve photon detection efficiency in the beam corridor, the lead glass beam detector was replaced by a copper/scintillator sandwich active degrader of larger diameter, also built at TRIUMF.

The TRIUMF-built central drift chamber (UTC) front end cathode pre-amplifiers and post-amplifier/discriminator electronics (768 channels) were replaced to overcome a problem associated with the cathode charge measurement system. As an additional benefit, improvements in the z position resolution along the wires were realized.

The energy, range, and decay sequence of charged particles are measured in the range stack scintillators. The two layers of limited-streamer mode straw tube tracking detectors within the RS were repaired and a new electronics front-end system was built and installed by the TRIUMF group. This resulted in greatly improved performance of the z-coordinate measurement used to suppress backgrounds from scattered muons.

After several months of parasite/shakedown operation, the initial data-taking for E949 took place during the period from mid-March to mid-June and delivered an exposure representing more than a third of E787's taken in one sixth of the time with higher relative sensitivity. Due to the problems with the AGS, the data were acquired at roughly twice the expected instantaneous rate and with the primary proton beam energy lowered from 24 to 20 GeV. Although most systems performed quite well, some problems arose with the upgrade of the central drift chamber cathode strip electronics system and the new beam hodoscope. These problems can be handled in the data analysis, but will be corrected in the hardware for the future.

Improvements were made to the reconstruction and calibration codes to combat high rates in the central drift chamber, and a double-pulse fit procedure for the CCD-digitized target fibre and beam counter pulses has been developed as well as an improved second-pulse-finding algorithm for the range stack.

In spite of strong endorsement of the science of E949 and myriad letters of support for the measurement by the world's leading scientists (including 15 Nobel Laureates), DOE funding for AGS running for E949 was curtailed in mid-2002. Various avenues of other funding for future running are being actively pursued.

KOPIO

The goal of KOPIO is to observe and measure the rate of the decay $K_L^0 \rightarrow \pi^0 \nu\bar{\nu}$. We aim to unambiguously detect a large sample of events so that η, the SM CP violation parameter, can be determined to 15% accuracy with minimal contributions from background or systematic effects. Like E787/E949, KOPIO has built-in redundancies and a reasonable level of contingency to meet the goal of a successful measurement.

In the KOPIO experiment, a 500 μsr solid angle neutral beam is extracted at 45° to produce a "soft" K_L spectrum peaked at 0.65 GeV/c; kaons in the range from about 0.5 GeV/c to 1.3 GeV/c will be used. Downstream of the final beam collimator is a 3.5 m long decay region which is surrounded by the main detector. Approximately 16% of the kaons decay yielding a decay rate of about 25 MHz. The beam region is evacuated to a level of 10^{-7} torr to suppress neutron induced π^0 production. The decay region is surrounded by an efficient Pb/scintillator photon detector which serves to veto photons and charged particles. In the forward detection region the primary photon detector system consists of two sections: a fine grained preradiator in which the photons are converted and the first e^+/e^- pair is tracked, followed by an 18 radiation length (X_0) calorimeter in which the remaining energy of the photon shower is measured. The preradiator measures the photon positions and directions accurately in order to allow reconstruction of the K_L decay vertex while also contributing to the achievement of sufficient energy resolution.

The preradiator is the main hardware responsibility of the Canadian group, and consists of 64 0.03 X_0 layers, each with plastic scintillator, metal converter and dual-coordinate drift chambers. Each preradiator layer consists of four flat square cell drift chambers (2 m $\times$ 2 m) with extruded Al comb backplanes and independent extruded scintillator elements read out by wavelength shifter (WLS) fibres.

R&D projects are proceeding well. A stack of 5 small (8 cm $\times$ 15 cm) KOPIO chambers has been constructed and is under test, and initial measurements gave the expected level of performance for efficiency and position resolution. Two medium size KOPIO chambers (30 cm $\times$ 30 cm) are operational for electronics development and specification. Two other chambers with full scale (2 m) in one dimension (anode or cathode) are under construction. The final prototype level will be a full size pre-production module of eight chamber layers.

The anode and cathode signals from each preradiator layer will be read out near the chambers. The electronics is designed to enable a fully pipelined deadtimeless system. Front end chamber electronics systems for both the anodes (including HV distribution) and cathodes have been tested on the development chambers. Multi-channel boards are being constructed and designs have been developed for the receiver and processor boards.

The extruded scintillator for the preradiator has proven to require additional R&D effort and expense and we are working with several potential suppliers (including a local plastics company) to achieve the light output and mechanical tolerances that are required.

The HERMES Experiment

(C.A. Miller, S. Yen, TRIUMF; M.C. Vetterli, SFU/TRIUMF; M.G. Vincter, Alberta)

The HERMES experiment was designed to comprehensively study the spin structure of the nucleon. It has been running at the HERA electron accelerator at the DESY Laboratory in Hamburg, Germany since 1995, measuring spin asymmetries for deeply inelastic electron scattering (DIS). The combination of a polarized high energy electron beam in a storage ring with undiluted polarized atomic gas targets is unique in this field, and has important experimental advantages. Furthermore, the spectrometer detecting the scattered electrons also has substantial acceptance and the capability to identify all types of hadrons produced in coincidence.

Inclusive spin structure functions

The original goal of the collaboration was to precisely determine the polarizations of the quarks of all flavours relative to the spin direction of the nucleon. This requires the combination of longitudinal spin asymmetries on both hydrogen and deuterium polarized targets. HERMES ran with a hydrogen target in 1996/7, and deuterium in 1998–2000. Based on the latter extensive data set, a preliminary extraction of the spin structure function g_1^d of the deuteron has now been released. Its unprecedented precision is illustrated in Fig. 13, where the structure function ratio g_1^d/F_1^d is shown as a function of Bjørken-x, which can be interpreted as the momentum fraction carried in the proton by the struck quark.

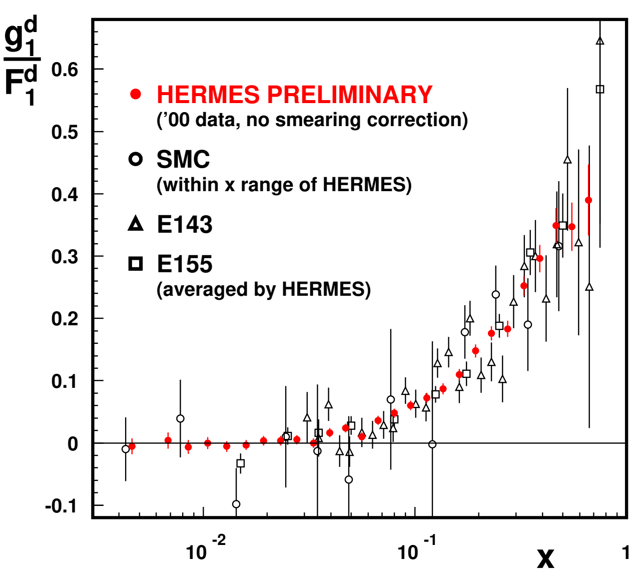

Fig. 13. Structure function ratio g_1^d/F_1^d for the deuterium target, which is closely related to the measured polarization asymmetry in inclusive DIS.

The comprehensive set of hyperfine transitions available in the atomic beam source providing the polarized deuterium for the target made it possible to also make the first measurement of the tensor spin structure function b_1^d. (Such a measurement is impractical with conventional solid polarized targets.) This structure function vanishes if the spin-one target is made up of spin-half nucleons at rest or in a relative s-wave. Our preliminary result from less than one month of running in tensor-polarized mode offers support for a model prediction based on a combination of a shadowing mechanism and the d-state component of the deuteron [Bora and Jaffe, Phys. Rev. **D57**, 6906 (1998)]. Figure 14 shows this result in the form of the structure function b_2, which is simply related to b_1 by the indicated relationship.

Quark spin densities from semi-inclusive DIS

A combination of inclusive polarized DIS data sets from both proton and deuteron targets is inherently limited to defining only the particular non-singlet combination of polarized quark distributions that is associated with the fundamental Bjørken sum rule. Further inferences from such data must be model-dependent. Quarks and antiquarks of the same flavour can not be distinguished since these cross sections scale as the square of the quark charge. To distinguish the contributions of the quark flavours and in particular of the sea quarks, it is necessary to use other types of

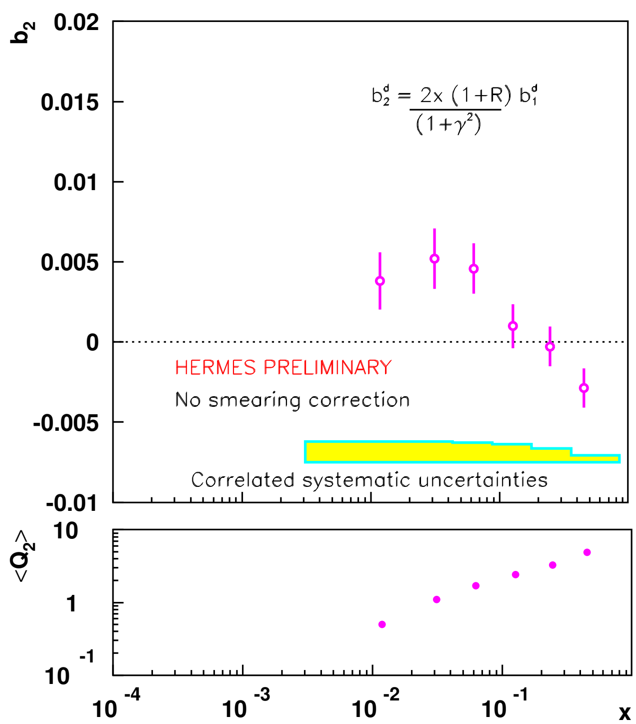

Fig. 14. The tensor spin structure function b_2^d on the deuteron target as measured for the first time by HERMES.

experimental information. In semi-inclusive scattering, a leading hadron is detected in coincidence with the deep-inelastic scattering of a lepton. This method exploits the correlation between the quark flavour and the type of leading hadron produced from the struck quark. Scattering asymmetries with various leading hadrons in the final state can be analyzed to determine the fractional contributions of the various quark flavours to the nucleon spin. Such an analysis uses data-constrained models for the fragmentation functions, which give the probability of a given flavour of quark to produce a given type of leading hadron.

The HERMES collaboration has released preliminary results for such a leading-order flavour decomposition from our complete data set recorded in the period 1996–2000. The data on the deuterium target recorded in 1998–2000 benefits from the dual-radiator Ring-Imaging Čerenkov detector (RICH) that identifies pions, kaons, and protons over the full momentum range. Hence kaon asymmetries are available for the first time, to provide sensitivity specific to the strange sea. The new preliminary results, now being prepared for publication, are shown in Fig. 15. They constitute the most precise information on quark helicity distributions, and for the first time provide separate determinations of the polarizations of the up, down and

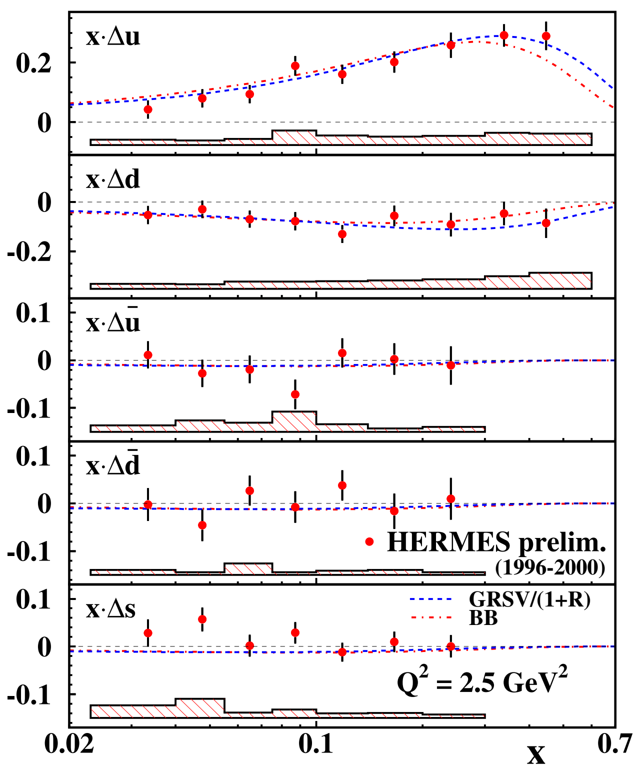

Fig. 15. Polarized quark distributions extracted from HERMES semi-inclusive 1996–2000 data sets. The curves are NLO QCD parametrizations of previous world inclusive data assuming SU(3) flavour symmetry.

strange sea quarks. They reveal that the sea quark polarizations are all small – there is little evidence of the "cancellation" between the contributions of valence and sea quarks that had been hypothesized to explain the small net contribution inferred from inclusive data under the assumption of SU(3) flavour symmetry. In particular, there is no indication that Δs is negative as indicated by that model-dependent analysis. Two theoretical groups are ready to perform next-to-leading-order analyses of these HERMES asymmetries.

The Canadian group played a major role in this analysis. For example, treatment of kinematic smearing by radiative and instrumental effects was done for the first time in this field by full unfolding, resulting in well-defined and quantitative (and small) correlations between data points.

Deeply virtual Compton scattering

The field of hadron structure has rapidly evolved in recent years. It is blessed with an extraordinarily dynamic community of QCD phenomenologists, who have essentially re-invented our view of hadron structure. All types of experimental observables are now integrated into the unified framework of generalized parton distributions (GPDs). Hard exclusive reactions have been identified as the key to further progress. Two features of this development promise to be revolutionary. If the GPDs can be sufficiently constrained by measurements of various observables for several hard exclusive reactions, it should be possible for the first time to determine the net contribution of parton orbital angular momenta to the nucleon spin. Deeply virtual Compton scattering (DVCS) is considered to be the most interpretable of these hard exclusive processes, as NLO QCD corrections and those for higher twist are already under theoretical control. Furthermore, the DVCS process has the unique virtue that it interferes with the well understood process of radiative elastic scattering from the nucleon target, fortuitously giving rise to a rich variety of large asymmetries in either beam or target polarization or beam charge, appearing in the azimuthal distribution of detected photons. This interference provides access to the DVCS scattering amplitudes. In analogy to the formation of holograms using such interference with visible light, images of the proton in the plane transverse to the beam can effectively be formed. In particular, the correlations between transverse coordinate (impact parameter) and momentum fraction of the partons can be measured. This technique of "femto-photography" has now been placed on a firm theoretical basis [Burkardt, submitted to Int. J. Mod. Phys. A, hep-ph/0207047; Diehl, Eur. Phys. J. **C25**, 223 (2002)].

To fully exploit these new possibilities will require the next generation of accelerator now being designed

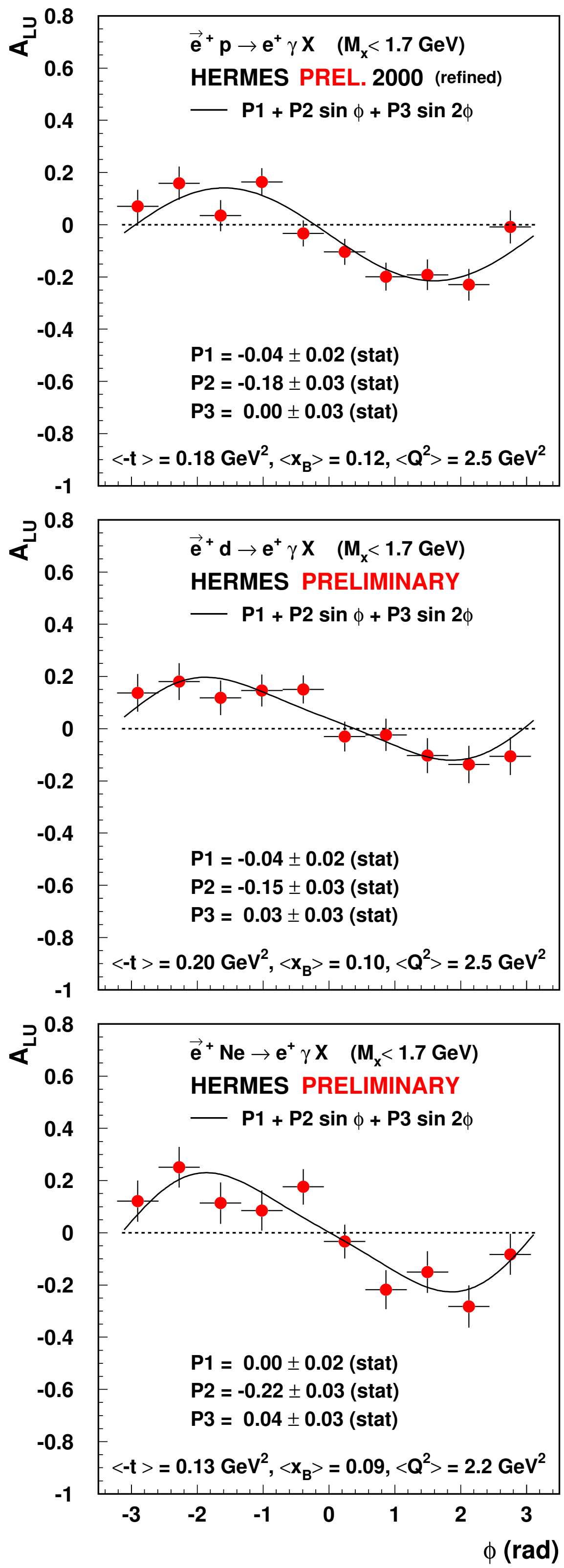

Fig. 16. Beam-spin asymmetries from DVCS/Bethe-Heitler interference on the three targets indicated, as a function of the angle of the detected photon azimuthally around the virtual-photon direction, relative to the lepton scattering plane.

for this purpose (e.g. e-RHIC at BNL, TESLA-N at DESY). However, HERMES now finds itself with the ability to make exploratory measurements that will guide this design. The first observation of a DVCS beam spin asymmetry was reported by HERMES in 2000. Now the collaboration has also recently released new and more precise DVCS beam-spin asymmetries for targets of hydrogen, deuterium and neon, based on the 2000 data set. Their azimuthal dependence for events selected in the kinematic region of the exclusive final state are shown in Fig. 16. Since the contribution of the coherent reaction on the deuteron is expected to be small, and the Bethe-Heitler cross section on the neutron is also small, the asymmetries for the proton and deuteron targets are expected to be similar, as is observed. On the other hand, the Z^2 amplification for the coherent reactions on neon makes this contribution important, as indicated by a more prominant peak in its t-distribution. An important reason for interest in the coherent reaction on nuclear targets is that the interpretation can be actually simplified in that the spin-flip amplitudes are suppressed by the preservation of the target ground state needed to allow the interference.

The above beam spin asymmetries constrain the imaginary part of certain DVCS amplitudes. The real part of these amplitudes is related to the asymmetry in the lepton beam charge. HERMES has recently released the first such measurement, shown in Fig. 17, revealing the expected cosine behaviour. The data are already able to discriminate among theoretical predictions corresponding to different choices for the

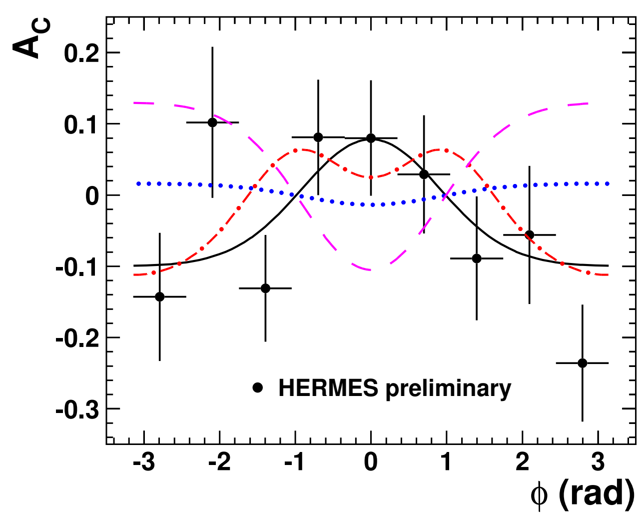

Fig. 17. Beam-charge asymmetries from DVCS/Bethe-Heitler interference on the hydrogen target. Three theoretical curves are shown; solid line: twist-2 + D term from a calculation in the chiral quark soliton model; dash-dotted: same calculation, but adding twist-3 effects; dotted: twist-2 without D term; dashed : same calculation as for solid line, but opposite sign for D term.

so-called "D term" in the generalized parton distribution, which is related to breaking of chiral symmetry. Refinements in the analysis that are presently under way will almost double the data available for this observable.

Asymmetries in the target spin are sensitive to other combinations of DVCS amplitudes. They have been extracted by a member of the TRIUMF group and have now been released. They indicate that the leading-twist $\sin\phi$ moment is small, but that the twist-3 moment $\sin 2\phi$ may be larger.

Single-spin azimuthal asymmetries

In 1999, HERMES and SMC released the first observations of semi-inclusive single-spin asymmetries that depend on the orientation of the hadron's momentum component $P_\perp$ azimuthally about the direction of the virtual photon. Relative to the lepton beam axis, the target polarization was transverse for SMC, and longitudinal for HERMES. In either case, the linear polarization of the virtual photon in the lepton plane selects transverse polarization of the struck quark. In leading twist and in this kinematic regime, $P_\perp$ can arise primarily from two sources: primordial p_T of the quark in the target, or k_T produced in the fragmentation process. A single-spin asymmetry requires the participation of some time-odd object correlating that p_T or k_T with some spin. Theoretical explanations of these asymmetries have focused on a T-odd fragmentation process sensitive to the transverse polarization of the fragmenting quark. The associated "Collins fragmentation function", designated $H_1^{\perp(1)}(z)$, is T-odd not in the fundamental sense, but only through the soft interactions in the final state. The wonderful implication of such an interpretation is that this "quark polarimeter" could provide access to the chiral-odd, and hence otherwise-inscrutable, transversity distribution. Transversity is the last remaining unmeasured one of the three leading-twist quark distributions that survive integration over intrinsic p_T. It is related to the probability of finding a transversely polarized quark in a nucleon polarized transversely with respect to its "infinite" momentum.

Unfortunately, almost all of the existing data revealing target-related single-spin asymmetries have been measured with a longitudinally polarized target. However, even these data can be interpreted in terms of the same Collins fragmentation function, operating together with transversity-related distribution functions – one twist-2 ($h_{1L}^\perp$, representing the probability of finding a transversely polarized quark in a longitudinally polarized nucleon) and one twist-3 (h_L). Hence such data from the HERMES collaboration, and now emerging from the CLAS collaboration at JLAB as well, offer important evidence that the Collins function has a substantial magnitude. However, there are presently too many unknowns for an unambiguous interpretation. Some assumptions must be made – e.g. neglecting either the interaction-dependent part of h_L, or neglecting $h_{1L}^\perp$ altogether. It has then been found possible to explain most of the existing data.

HERMES has now also released results on the same observable for both pions and kaons from a deuterium target. Selected examples of these data are shown in Fig. 18, and compared to theoretical predictions where

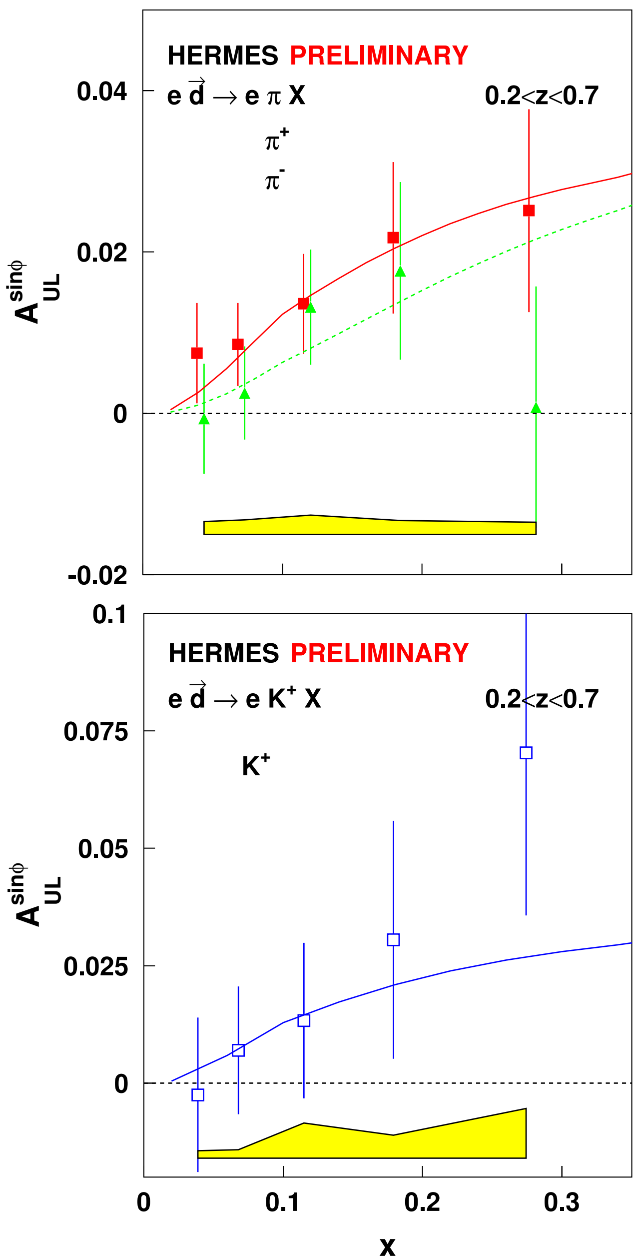

Fig. 18. Preliminary HERMES analyzing powers in the $\sin\phi$ moment of single-spin asymmetries with a longitudinally polarized deuterium target, as a function of Bjørken x. The curves are theoretical calculations [Efremov *et al.*, Eur. Phys. J. **C24**, 407 (2002)].

the transversity distributions are calculated in the chiral quark soliton model. In these calculations, the interaction-dependent part of h_L was neglected. The Collins function was parametrized to fit the HERMES proton data, now resulting in a magnitude which corresponds to the "optimistic" (large) extreme from a Delphi preliminary analysis of $e^+e^- \to 2$ jets: $\frac{\langle H_1^{\perp(1)} \rangle}{\langle D_1 \rangle} = (12.5 \pm 1.4)\%$. Previous estimates of the Collins function were only half this size, due to a theory-error in the sign of the contribution of that component of the target polarization that is orthogonal to the virtual photon direction. (This component appears even in the HERMES experiment with target polarization parallel to the lepton beam.) Another result of the corrected sign is that the sign of the SMC preliminary asymmetry with a transversely polarized target no longer appears to be theoretically consistent with that of the HERMES results with a longitudinally polarized target, although those SMC data are not statistically definitive.

Work by others is now under way to extract the Collins function from Belle e^+e^- data. This information can be used to interpret new data now being recorded by HERMES with a transversely polarized hydrogen target, in order to extract the quark transversity distribution.

Other results in spin physics

Space here does not permit an adequate summary of other new HERMES results related to spin physics. For example, using the polarized proton data, quark-hadron duality has been demonstrated for the first time in a spin asymmetry [Airapetian *et al.*, hep-ex/0209018]. Also an unprecedented and complete determination of the generalized Gerasimov-Drell-Hearn (GDH) integrals for the proton, deuteron and neutron was made over the range in exchanged photon virtuality $1.2 < Q^2 < 12.0\,\mathrm{GeV}^2$ and for photon-nucleon invariant mass squared W^2 ranging over $1 < W^2 < 45\,\mathrm{GeV}^2$, thus covering both the nucleon-resonance and DIS regions [Airapetian *et al.*, hep-ex/0210047]. No departure from leading-twist behaviour appeared over this entire kinematic range.

Quark fragmentation in the nuclear environment

The standard HERA operating procedure allows the routine use of thick unpolarized targets for higher luminosity (up to $3 \times 10^{33}\,\mathrm{cm}^{-2}\,\mathrm{s}^{-1}$) for one hour at the end of each beam fill. (This has been the main source of most of the data for the DVCS beam-related asymmetries.) In addition, various gaseous nuclear targets have been employed to study the hadronization process in the nuclear environment, through the measurement of nuclear attenuation of the multiplicity of identified hadrons. Such unique data from HERMES have been analyzed to extract the rate of energy loss of partons in the nuclear medium. In one approach [Wang, Nucl. Phys. **A702**, 238 (2002)], the effect of gluon Bremsstrahlung induced by multiple scattering of a highly off-shell quark and the resulting parton energy loss is expressed in terms of in-medium modification to the quark fragmentation functions. This analysis is based on the original recognition that this soft gluon radiation is coherent in the sense of the LPM effect in QED [Baier *et al.*, Phys. Lett. **B345**, 277 (1995)], and that therefore the energy loss is remarkably proportional to the square of the distance in the medium [Baier *et al.*, Nucl. Phys. **B484**, 265 (1997)]. The A-dependence of the HERMES attenuation data supports this prediction, and not alternate models in which e.g. the attenuation is largely caused by ordinary nuclear absorption of either the QCD string stretched by the struck quark or subsequent absorption of the formed hadron. The Wang model employs the HERMES data to interpret observations of jet quenching in collisions of relativistic nuclei at, for example, RHIC.

Colour transparency

Among other new results from nuclear targets is the first clear evidence in lepton scattering of the effects of the phenomenon of colour transparency, in diffractive ρ^0 production on nuclei. Mesons produced by photons with large virtuality exist initially as "small-size configurations", and experience less attenuation in traversing the nuclear medium. The resulting paper has been accepted in Phys. Rev. Lett. [Airapetian *et al.*, hep-ex/0209072].

The ongoing HERMES program

DESY has promised beam for HERMES until at least the end of 2006. The plan that is approved by the DESY Physics Review Committee is to spend until the end of 2004 on a transversely-polarized hydrogen target to make the first measurement of quark transversity. (This intent was mentioned in the original proposal; since then a single-spin asymmetry that HERMES discovered revealed a suitable experimental signal.) This may also result in the first observation of a particular time-odd distribution function, which until very recently was thought to be excluded by basic time reversal invariance. It is expected there will be enough statistics for a preliminary result by the start of the 4-month HERA shutdown in March, 2003.

Meanwhile, HERMES is designing and constructing a new recoil detector to surround the target cell and detect the recoiling intact target nucleon from hard exclusive processes, in order to guarantee their exclusivity. This fully funded €1.4 M project is scheduled to be ready for two years of running on high density unpolarized targets in 2005/6. This will yield the first really high quality data on asymmetries in both beam spin and charge for DVCS, the process that holds the most promise to shed light on the orbital angular momentum of partons.

HERMES collaborators in 2002: G. Gavrilov, J. Lu, C.A. Miller, S. Yen (TRIUMF); M.V. Vetterli (SFU/TRIUMF); M.G. Vincter (Alberta); K. Garrow (Alberta/SFU); J. Wendland (SFU).

KEK Expt. 246 and 470 (Japan-Russia-Canada-Korea-U.S.A. Collaboration)
Kaon decay studies

(M.D. Hasinoff, UBC; J.A. Macdonald, B. Shin, TRIUMF)

The KEK apparatus [Abe *et al.*, submitted to Nucl. Instrum. Methods A] at the 12 GeV Proton Synchrotron (PS) for the search for T-violation in the transverse polarization (P_T) of muons in $K^+_{\mu 3}$ decay has been demonstrated to be well suited to precision studies of other kaon decay modes, e.g., $K^+_{\pi 3}$ [Shin *et al.*, Eur. Phys. J. **C12**, 627 (2000)], K^+_{e3} [Shimizu *et al.*, Phys. Lett. **B495**, 33 (2000)] and $K^+_{\mu 3}$ [Horie *et al.*, Phys. Lett. **B513**, 311 (2001)]. The detector consists of an active scintillating-fibre target which serves as a kaon stopper and vertex detector, a CsI(Tl) calorimeter system which detects photons including π^0 decay, and a superconducting toroidal magnet spectrometer system to analyze and select μ^+s e^+s, and π^+s. A muon polarimeter system is located at the quasi-focal planes of the toroidal magnet gaps. The complete kinematics from stopped K-decay can be reconstructed from the charged track obtained in the target, ring scintillators and spectrometer tracking chambers, and from photons and π^0s in the photon detector array.

Data-taking for the T-violation search was completed in 2000. In 1999, after the analysis of data taken in 1996 and 1997, we reported a value for P_T in $K_{\mu 3}$ of $-0.0042 \pm 0.0049(\text{stat}) \pm 0.0009(\text{syst})$ and $\text{Im}(\xi) = -0.013 \pm 0.016(\text{stat}) \pm 0.003(\text{syst})$ [Abe *et al.*, Phys. Rev. Lett. **83**, 4253 (1999)]. The analysis effort since then has been directed at the total data set taken 1996–2000. The strategy has been to undertake two independent analyses in order to check for errors and biases. In 2002, the first of the two analyses was completed and a new result was reported at the PANIC 2002 conference in Osaka [Abe *et al.*, hep-ex/0211049 (2002)]. This new result, $P_T = -0.00112 \pm 0.00217(\text{stat}) \pm 0.0009(\text{syst})$ and $\text{Im}(\xi) = -0.0028 \pm 0.0069(\text{stat}) \pm 0.003(\text{syst})$, remains consistent with the standard model expectation of no T-violation, and should be considered preliminary until the second analysis is completed. The latter is in the final stages and is expected to be complete in early 2003. Additional analytical techniques are being used in order to better deal with systematic effects related to the stopping distribution of the kaons in the target and the muons in the polarimeter.

In October, 2001, the last beam time with the apparatus was used to study the radiative $K_{\pi 2}$ decay, $K^+ \to \pi^+ \pi^0 \gamma$. This decay channel is unique, in which the direct photon emission from the vertex is easy to observe because the internal bremsstrahlung contribution is suppressed by the $\Delta I = 1/2$ rule. This direct emission is dominated by the chiral anomaly of magnetic transitions and the decay amplitude can be analyzed in terms of chiral perturbation theory (ChPT).

For this run, additional photon veto counters were added to detect photons escaping through the muon holes in the CsI(Tl) calorimeter, and the trigger demanded the presence of 3 photons in the calorimeter.

In 2002 the analysis was completed. The π^+ was distinguished from μ^+s and e^+s by time of flight. Most of the non-radiative $K_{\pi 2}$ two-body decays were excluded by momentum analysis. The difficult task of pairing the correct two photons to the π^0 was done by detailed kinematic analysis of the three possibilities. To extract the direct emission branching ratio, the detector response was simulated in GEANT3 and tested against the $K_{\pi 2}$ two-body decays. This measurement extends the recent result from BNL E787 [Adler *et al.*, Phys. Rev. Lett. **85**, 4856 (2000)] by virtue of its high kinematic resolution, and its capability to reach the lower π^+ energy region, $T_\pi > 35$ MeV where the direct photon emission is more important. Our result [Aliev *et al.*, Phys. Lett. B, in press] confirms the BNL result when the partial branching ratio for the π^+ kinematic region is taken into account. No evidence was found for an interference component between the direct photon emission and the dominant inner bremsstrahlung, which indicates the pure magnetic nature of direct emission in $K_{\pi 2\gamma}$ decay.

In early 2002, the apparatus was removed from the K5 channel at the KEK PS to make way for other experiments. Letters of Intent for a new T-violation experiment and for kaon decay spectroscopy of interest to members of the collaboration have been prepared for future extensions of this work at the J-PARC facility now under construction.

Sudbury Neutrino Observatory

(R. Helmer, TRIUMF)

Data-taking with salt in the heavy water continued throughout the year. As reported in last year's Annual Report, there is little need for TRIUMF infrastructure support at the present time. A small part for one of the calibration sources was designed in the Design Office and fabricated in the Machine Shop.

In the meantime, SNO reported an extremely important result; namely, solid evidence showing that electron neutrinos produced in the sun transform to another active flavour during their transit to earth. Specifically, the flux of electron neutrinos was found to be

$$\phi(\nu_e) = 1.76 \pm 0.05(\text{stat}) \pm 0.09(\text{syst}) \times 10^6\ \text{cm}^{-2}\text{s}^{-1}$$

while the flux of active, non-electron neutrinos was found to be

$$\phi(\nu_{\mu\tau}) = 3.41 \pm 0.45(\text{stat})^{+0.48}_{-0.45}(\text{syst}) \times 10^6\ \text{cm}^{-2}\text{s}^{-1},$$

5.3 σ greater than zero. The total flux, measured with the neutral current reaction, was found to be

$$\phi(\text{NC}) = 5.09^{+0.44}_{-0.43}(\text{stat})^{+0.46}_{-0.43}(\text{syst}) \times 10^6\ \text{cm}^{-2}\text{s}^{-1},$$

consistent with solar models.

The day and night energy spectra measured with SNO were reported in a second publication. The night minus the day rate was found to be $14.0\% \pm 6.3\%(\text{stat})^{+1.5\%}_{-1.4\%}$ of the average rate, and the asymmetry in the flux of electron neutrinos was found to be $7.0\% \pm 4.9\%^{+1.3\%}_{-1.2\%}$, assuming the flavour transformation was to active neutrinos only. A global analysis using all other solar neutrino data, including SNO's day and night energy spectra, strongly favoured the large mixing angle solution of the solar neutrino problem.

TJNAF Experiment 00-006
Measurement of the flavour singlet form factors of the proton (*G*∅)

(W.T.H. van Oers, Manitoba)

The detailed structure of the nucleon at low energies is not well understood within the framework of quark and gluon degrees of freedom. For example, relatively little is known about the importance of the sea quarks at these energies. The $G\emptyset$ experiment will measure two proton ground state matrix elements which are sensitive to point-like strange quarks and hence to the quark-antiquark sea in the proton. The matrix elements of interest are the elastic scattering vector weak neutral current charge and magnetic form factors, G_E^Z and G_M^Z, respectively. These can be extracted from a set of parity-violating electron-proton scattering measurements. If one assumes a relationship between the proton and neutron structure in that the proton and neutron differ only by the interchange of up and down quarks, i.e., isospin symmetry, the strange quark (as well as the up and down quark) contribution to the charge and magnetic form factors of the nucleon can be determined. This would result from taking appropriate linear combinations of the weak neutral form factors and their electromagnetic counterparts.

Determinations of both the charge and magnetic strange quark form factors are of fundamental interest, as these would constitute the first direct evidence of the quark sea in low energy observables. It is the objective of the $G\emptyset$ experiment to determine these contributions to the proton form factors at the few percent level. Observations at high energy suggest that the strange quarks carry about half as much momentum as the up and down quarks in the sea. It is important to determine both the role of the quark sea and the relevance of strange quarks at low energy where there are voids in understanding the theory of the strong interaction (quantum chromodynamics, QCD). Even if the strange quark contributions are found to be below the sensitivity level of the experiment, upper limit determinations are as valuable as non-zero results. The matrix elements, G_E^Z and G_M^Z, are also relevant to discussions of the Ellis-Jaffe sum rule and the pion-nucleon sigma term; there is uncertainty in both of these about the strange quark contributions. The $G\emptyset$ experiment will allow the determination of the strange contributions to the proton charge and magnetic form factors in a more straightforward manner.

In the $G\emptyset$ experiment, which is being carried out at the Thomas Jefferson National Accelerator Facility (TJNAF), parity-violating longitudinal analyzing powers will be measured in electron-proton scattering in the range $0.1 \leq Q^2 \leq 1.0$ GeV^2 at both forward and backward angles. The longitudinal analyzing power is defined as

$$A_z = (1/P)\frac{[\sigma^+(\theta) - \sigma^-(\theta)]}{[\sigma^+(\theta) + \sigma^-(\theta)]}$$

where P is the polarization of the incident electron beam and the + and − signs indicate the helicity state. Making pairs of measurements at forward and backward angles will allow the separation of G_E^Z and G_M^Z. Predicted longitudinal analyzing powers range from about $(-3$ to $35) \times 10^{-6}$; it is planned to measure the longitudinal analyzing powers with statistical uncertainties of $\Delta A/A = 5\%$ and systematic uncertainties related to helicity correlated effects of $\Delta A/A \leq 2.5 \times 10^{-7}$. In the first phase of the experiment, longitudinal analyzing powers will be measured concurrently at several values of the momentum transfer in the range $0.1 \leq Q^2 \leq 1.0$ GeV^2. It now also appears that higher beam polarizations (∼70%) will be available at the reduced beam pulse frequency of 31 MHz, decreasing the original estimate of 700 hours for the first phase of the experiment. However, it must be realized that the length of the experiment is in part governed by making rather elaborate control measurements to determine the corrections that have to be made to the measured asymmetries and to assess systematic errors. In the second phase of the experiment, each subsequent backward angle analyzing power measurement would require from one half to one month of running time. The results of the SAMPLE experiment at the MIT-Bates Laboratory have shown the importance of measuring the axial form factor corrections, since these appear to be quite different from the theoretical predictions. Therefore, companion measurements of quasi-elastic scattering from deuterium will also be made at the backward angles. With these measurements, the effective axial current of the nucleon will also be determined. This current includes effects from the effective axial coupling of the photon to the nucleon or anapole moment, which are relevant also in other processes, e.g., parity violating Moller scattering and atomic parity violation.

The $G\emptyset$ collaboration

The $G\emptyset$ experiment is being carried out in Hall C at TJNAF by a collaboration of scientists from Canada, France, Georgia, and the United States, with funding provided through NSERC (Canada), IN2P3 (France), and DOE/NSF (US).

This past year has seen the completion of many critical milestones for the experiment. The apparatus for the forward angle measurements is now installed in Hall C and a first set of commissioning runs with beam was carried out from August, 2002 to January, 2003. As well, considerable progress has been made in the design, prototyping, and fabrication of critical components for the second phase backward angle mode of the experiment. The Canadian contributions to these efforts have been significant.

Canadian contributions

The Canadian members of the $G\emptyset$ collaboration, based at the Universities of Manitoba, Northern British Columbia, and TRIUMF, have been asked to:

(1) Develop and produce specialized photomultiplier tube bases for the main detector arrays;
(2) Design, build, and commission an automated magnetic field measuring apparatus complete with its own data acquisition system;
(3) Prototype and fabricate the cryostat exit detector arrays for the backward angle measurements;
(4) Prototype and fabricate (together with the Grenoble group) the aerogel Čerenkov arrays for background rejection in the backward angle measurements;
(5) Design the support structure for the aerogel Čerenkov and cryostat exit detector arrays;
(6) Coordinate the implementation of TJNAF built beam monitors and control apparatus with TRIUMF-built parity electronics;
(7) Provide design and implementation support for the liquid hydrogen target slow controls system;
(8) Provide support for the coordinating and scheduling of resources for $G\emptyset$ commissioning and engineering runs at TJNAF.

Much progress has been made in the design and construction of the various subsystems listed above, many of which are now in operation.

Photomultiplier tube bases

The heart of the $G\emptyset$ detection system is a spectrometer which consists of an eight-sector toroidal magnet, with an array of scintillation detectors located at the focal surface of each sector (see Fig. 19). Since data will not be acquired in event-by-event mode in this experiment, and since the scintillator arrays are the only detectors to measure the scattered particles in the forward angle mode, the performance of these focal-plane detectors (FPD) is of critical importance. The timing and pulse shape characteristics of this system must be fine-tuned at the hardware level as it will not be possible to reconstruct individual events. Furthermore, the rates associated with many of the FPD elements will be quite high (1 MHz) and the photon yield(s) will have a large dynamic range. As such, special demands will be made on the photomultiplier tubes (PMT) and especially on their associated divider/base circuit. The design, development, and building of the $G\emptyset$ bases (for the North American FPD arrays) was carried out at TRIUMF. Several iterations of prototype high-rates bases were constructed at TRIUMF and tested at TJNAF, and in mid-1998, a set of final prototype bases was constructed and delivered to TJNAF for tests with the first set of prototype FPDs. Fabrication of the production bases began shortly thereafter. With the help of summer students (funded partly through the TRIUMF Summer Students program and partly through the $G\emptyset$ NSERC grant), the fabrication of the electrical components for all of the production bases was completed in late 1998. The design of the mechanical housing for the PMT-base subsystem depended on

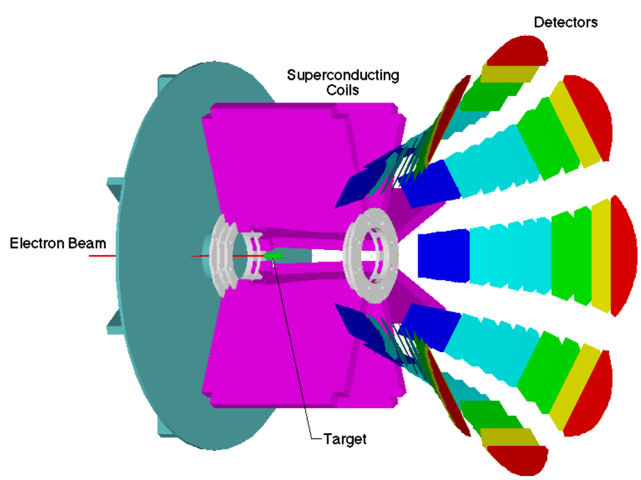

Fig. 19. Schematic layout of the $G\emptyset$ spectrometer.

the final design of the FPD support structure and, after much effort resolving subsystem integration issues, the final design for the PMT-base housing assembly was completed in late 1998. The fabrication and assembly of the mechanical housings and integration of the electrical components was completed over the summer of 1999 (again with the help of summer students at TRIUMF). Final testing of the completed bases was carried out in the fall of 1999, and shipment of all the bases (300 units) to TJNAF occurred at the end of calendar year 1999. Integration of this subsystem with the FPD arrays and the DAQ electronics, was completed at TJNAF in 2000 and 2001 during the final assembly of the FPD system. Presently, all of the FPDs are fully instrumented and have undergone tests of the detector "chain" (scintillator/PMT-base/electronics/DAQ/analysis) in Hall C using cosmics, beam background and, as of this summer, $G\emptyset$ test beam during the first sets of commissioning/beam-development runs.

Magnetic verification

An automated field measuring apparatus was constructed to provide a magnetic verification of the $G\emptyset$ superconducting toroidal magnet by determining the locations of a pre-specified set of magnetic reference points. These reference points correspond to the zero-crossing locations of specific field components at selected points of symmetry around the toroidal magnet, and they are a sensitive function of the coil positions. Determination of these zero-crossing points then allows the actual coil positions and, in principle, the magnetic fields to be completely determined. The measurements are carried out by scanning over a predefined set of zero-crossing lines, and determining where specific field components reverse signs. The system must be capable of providing a position determination of $\pm$ 0.2 mm and a field determination of $\pm$ 0.2 G, in order to reach the design goal of $\pm 0.2 - 0.3$ mm for the zero-crossing determination. Considerable effort went into the design, construction and commissioning of this magnetic field measuring apparatus or magnetic verification device at TRIUMF, the University of Manitoba and UNBC. The device consists of a programmable gantry with full 3D motion anywhere within a 4 m $\times$ 4 m $\times$ 2 m volume, and a set of high precision Hall probes, thermocouples, and clinometers (which measure tilt-angles) is mounted at the end of a probe boom on the gantry (see Fig. 20). Procurement of parts commenced in early 2000, and final assembly and testing began in late spring, 2000. With the support of TRIUMF Engineering and the TRIUMF summer/co-op student program, the magnetic verification device was completed in mid-summer, 2000 and transported to the University of Illinois (UIUC) where the magnetic measurements would be carried out. In late 2000 and early 2001, much effort went into commissioning this device at UIUC and upgrading and modifying the motion control and data-acquisition software. In the spring of 2001, a series of test measurements were carried out with the magnet energized at room temperature and very low currents. The magnetic verification device yielded remarkably consistent results. Shown in Fig. 21 is the magnetic verification device and the $G\emptyset$ superconducting spectrometer.

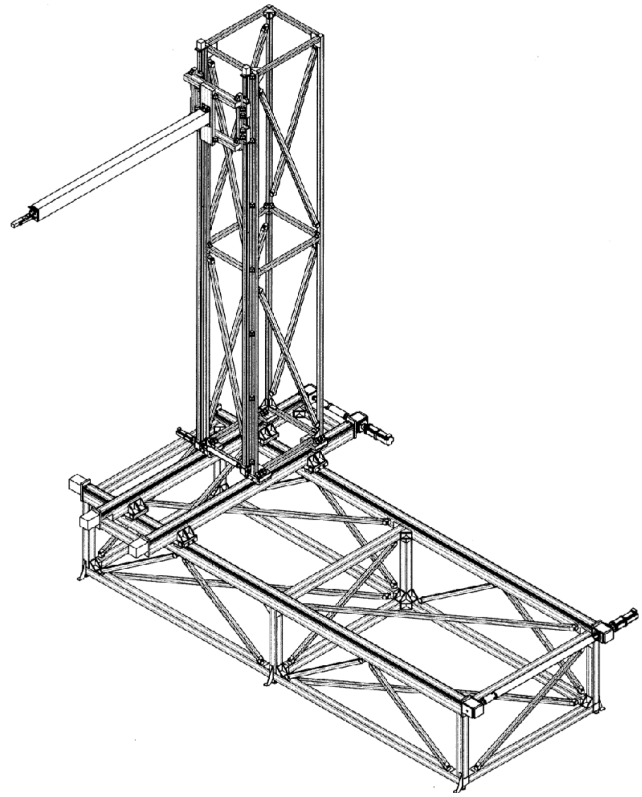

Fig. 20. Layout of the magnetic verification apparatus.

In late 2001, after significant effort by the UIUC group to cool the $G\emptyset$ magnet to superconducting temperatures, the transition to superconducting mode was achieved and a set of magnetic field measurements was carried out. Due to limited cooling capacity and other magnet-related difficulties, the magnetic verification measurements were carried out with the coils energized at 1000 A (20% of the full-field value) and only a subset of the scans could be performed. Three sets of background magnetic field measurements were made, interleaved with two sets of foreground magnetic field measurements at 1000 A. In all, 30 zero-crossing points were scanned for each magnet sector, for a total of 240 zero-crossing values per data set. Preliminary processing of these data involved applying corrections for: Hall probe offsets and the background magnetic field; clinometer readings; and Hall probe

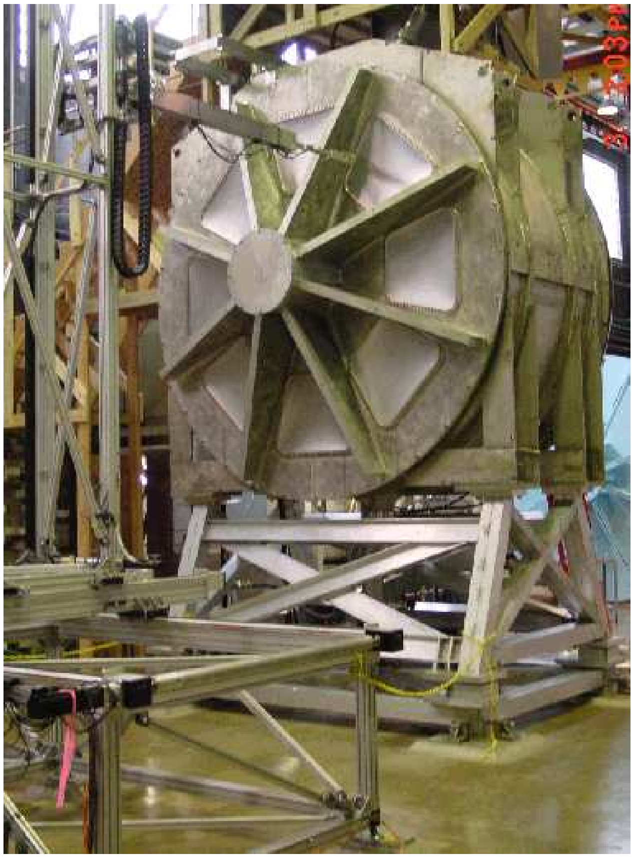

Fig. 21. The magnetic verification apparatus and $G\emptyset$ superconducting magnet at UIUC.

misalignments. Various combinations of these corrections were applied and a total of 18 different raw data sets were generated. The zero-crossing points of the various field components were subsequently determined for each of these 18 different data sets. Measured uncertainties associated with these zero-crossing points varied widely, depending on the particular location of the scan. Typical errors were ± 0.15 mm, but in regions where the field gradients were small (down an additional factor of 5 due to the lower magnet currents) the errors were significantly larger.

The analysis procedure used to extract the coil positions from the zero-crossing points was tested against computer simulations, where known coil displacements were used to generate simulated data. Not only were the displaced coil positions correctly extracted, but the relative orientations and positions of the Hall probes themselves could also be extracted. This was due in part to the symmetry of the set-up and the large number of zero-crossing points involved. Analysis of the actual experimental data quickly revealed that the gantry frame was offset with respect to the toroid frame by about $\delta X = 0.62$ cm and $\delta Y = -0.33$ cm. Allowing the analysis procedure to correct for this resulted in the residual coil displacements shown in Fig. 22. Most

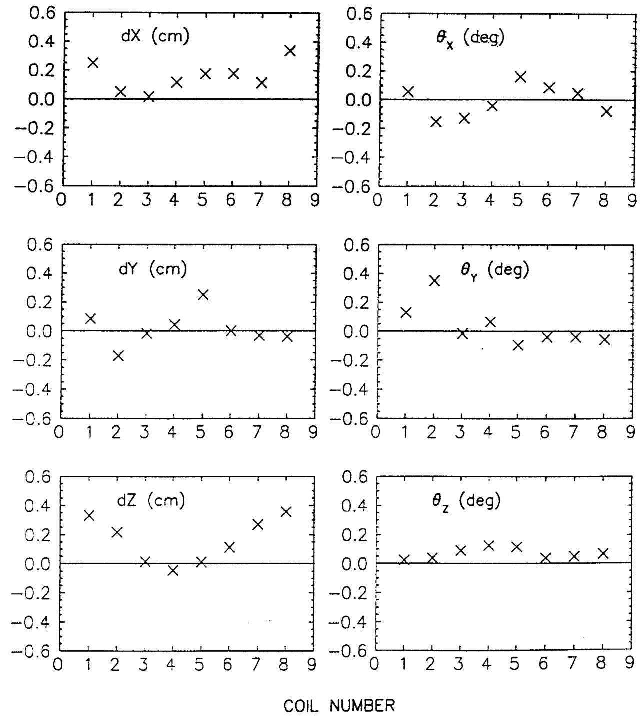

Fig. 22. Coil displacements for the $G\emptyset$ toroid extracted from the zero-crossing data.

of the angular displacements were about $0.1°$, and the linear displacements less than 0.2 cm. This was well within the specifications for the tolerances on the coil positions laid out in the original design. The behaviour of dZ required further study. The shape of the curve suggested that the $X - Y$ plane mapped out by the gantry (with constant Z) was not parallel to the toroid $X - Y$ plane. A value of $0.11°$ was extracted for this angle between the planes. In addition, the fact that all (except for coil 4) dZ values were positive, suggested that there was also an offset in the Z-coordinate between the gantry and toroid frame. Indeed, further analysis revealed that the experimental data recorded with a Z-coordinate of 187 cm were actually recorded at 185.95 cm. When the magnet endcaps were later removed during repairs at the University of Illinois it was observed that the coils were closer to the downstream endcap by about 1/2 in., in good agreement with the 1.05 cm found above.

It should be noted that, although this magnetic verification device was designed, built, and tested by the Canadian subgroup at TRIUMF and the Universities of Manitoba and Northern BC, funding for hardware components of this subsystem was provided by NSF through the University of Illinois. Infrastructure support, however, has been provided by TRIUMF and the Universities of Manitoba and Northern British Columbia.

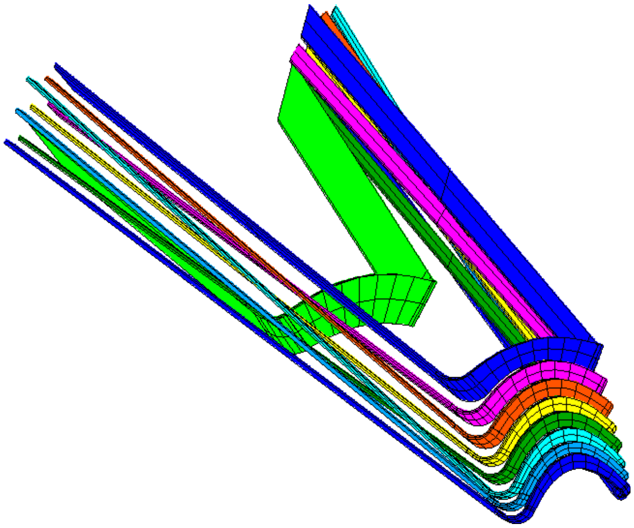

Fig. 23. Layout of a cryostat exit detector (CED) array for a single octant.

Cryostat exit detectors

For the backward angle measurements during the second phase of the $G\emptyset$ experiment, the addition of a second array of scintillation detectors, located near the spectrometer-cryostat exit windows, will be required in order to separate the elastic and inelastically scattered electrons. The geometry of these cryostat exit detector (CED) arrays (see Fig. 23) has been studied in detail and a reference design was completed in 1999. With the resident expertise at TRIUMF in producing high quality scintillation detectors and lightguides, the Canadian subgroup was asked to play the main role in the prototyping and production of the CEDs. A set of prototypes was built at TRIUMF and delivered to Louisiana Tech. University for further studies in 1999. Results from these studies indicated that the reference design and the prototype detectors met the specification requirements for the CED arrays. Production of a full set of dummy CED prototypes was then completed at TRIUMF in 2000, to aid in the design of the CED support structure. After finalizing the CED design, construction of the production versions of the CED arrays began in late 2000. Fabrication of the CED scintillators for all 8 octants was completed and delivered to TJNAF in late 2001, and fabrication of the special helical-bent lightguides began in 2002. In order to achieve the unique helical bend required in the $G\emptyset$ back angle geometry, customized bending jigs were designed and constructed at TRIUMF and tested on a first set of CED lightguides. Production of the lightguides is presently nearing completion and delivery to TJNAF is scheduled for summer, 2003. The CEDs will also make use of the same types of photomultiplier tubes and specialized TRIUMF/$G\emptyset$ bases as the FPDs.

Aerogel Čerenkov detectors

Monte Carlo simulation results have shown that backgrounds from negative pions will be problematic for the second phase backward angle measurements involving the deuterium target. The $G\emptyset$ simulation subgroup has focused on characterizing this π^- background and providing options regarding the design of an additional set of detectors to reject the background pions. The $G\emptyset$ Canadian and French (Grenoble) subgroups have been asked to jointly undertake the prototyping and construction of this crucial set of detectors, which will be made up of an array of aerogel Čerenkov counters. Much effort has gone into the design of this detector array and a conceptual design (see Fig. 24) was evolved into a first prototype at TRIUMF.

Prototype tests using the TRIUMF pion beam (M11) were carried out in December, 2001, but were hampered by the fact that there was insufficient aerogel to fully load the detector, which led to inconclusive results. This situation was rectified in early 2002, and further tests using cosmic rays were carried out at TRIUMF over the spring and summer of 2002. Issues that have been studied include: the optimal choice and configuration of reflective material within the light diffusion box; the choice of photomultiplier tube (PMT) and base; the best procedure to establish a hit (summed signal vs. multiplicity); characterization of the diffusion box response by Monte Carlo

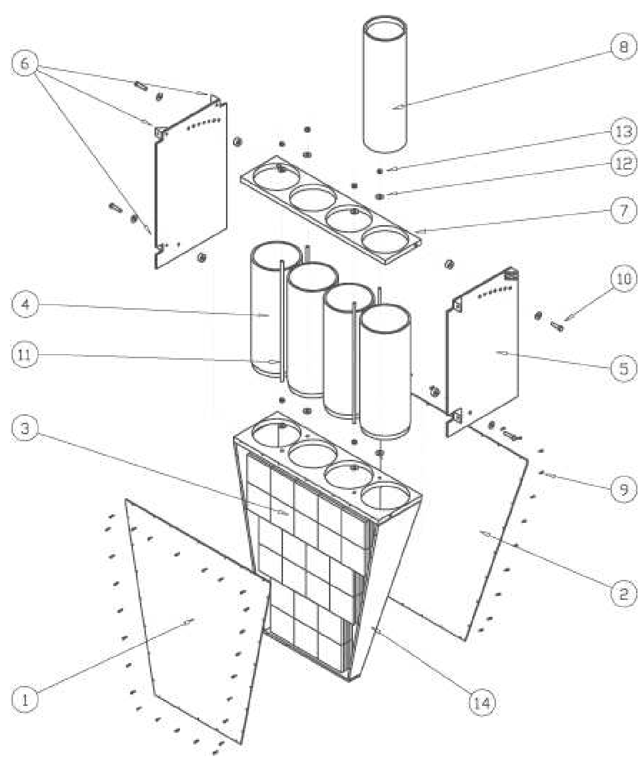

Fig. 24. Conceptual layout of aerogel Čerenkov detector.

simulations; magnetic shield requirements; radiation shielding requirements; and optimization of the solid angle of the detector.

In the recent tests with cosmic rays, different PMTs were tested in the detector box and the choice, thus far, is to retain the Photonis XP4572B. Millipore paper was chosen as the diffuse reflector in the box. Most of the inner surfaces of the box were lined initially with an underlayer of Tyvek and one layer of millipore. Later, a second layer of millipore was added. The collars around the PMTs were also lined with millipore. Measurements were made at different positions: (i) near the PMTs, (ii) at the centre of the box, and (iii) far from the PMTs, where, it should be noted, there were only four stacked aerogel tiles (as opposed to five in the rest of the box active area). Shown in Fig. 25 are ADC spectra for the summed pulse height of the four tubes for the three positions listed above.

Another issue, related to the inactive region of the photocathode around the PMT front face, was studied in detail. A reflective cone was designed to cover this region and to redirect the light toward the active portion of the PMT photocathode. Different reflective materials on this cone were tested, including an experimental reflective (dichroic) film from 3M (claimed to be a very efficient reflector at 320 to 430 nm). Although results with the dichroic reflector were initially encouraging, it was later demonstrated that good quality (thicker) aluminized mylar resulted in comparable or even slightly better detector efficiencies. The measured relative efficiency for cosmics passing near the centre of the detector is approximately 90% and 85%, for single- and two-photoelectron thresholds, respectively. Studies of light propagation in the diffusion box are also being carried out using the programs LITRANI, GEANT4, and a simple Monte Carlo.

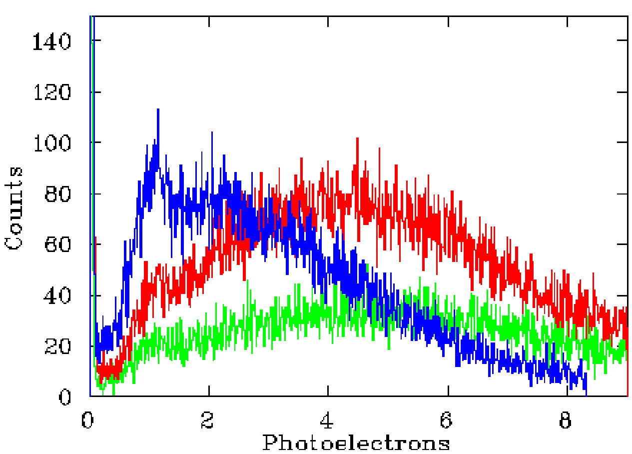

Fig. 25. Pulse height spectra for the four-PMT summed signal for 3 trigger positions: (i) near the PMTs [green], (ii) near the detector centre [red], and (iii) far from the PMT [blue].

Further in-beam tests with the prototype Čerenkov detector were carried out in December, 2002 using the M9 beam line at TRIUMF and the data are currently being analyzed. A second iteration prototype is also presently being designed.

Backangle support structure

Considerable effort has gone into the engineering design of a support structure for the Čerenkov and CED arrays. Although the Canadian subgroup was initially responsible only for the design of the Čerenkov support structure, it was soon realized that the CED support structure would be closely coupled to the former due to the physical proximity of the two detector subsystems. As such, an integrated design for the two detector subsystems is presently being pursued. The support structure will centre around the use of prefabricated aluminum extrusions from Bosch because of their strength, versatility, and relatively low costs. A series of detailed finite-element analysis studies have been carried out at TRIUMF, using the program ANSYS, to identify potential problems and to optimize the strength/cost of the support structure. The present design consists of a second Ferris wheel type support structure, which is to couple to the existing FPD support structure (also a Ferris wheel type design) and to the linear rails on the existing $G\emptyset$ detector platform. A conceptual illustration of the $G\emptyset$ backward angle configuration is shown in Fig. 26, with the superconducting magnet, the 3 detector arrays (FPD, CED, Čerenkov) in each of the 8 sectors, and their respective support structures.

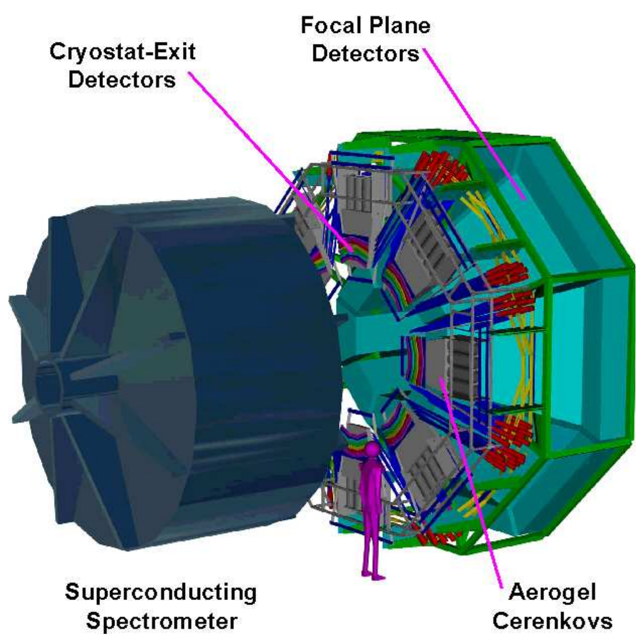

Fig. 26. Conceptual layout of the $G\emptyset$ backward angle configuration.

Beam line monitors

The success of the $G\emptyset$ experiment will be closely linked to the precise measurement and control of the electron beam properties. To make the subtle, refined asymmetry measurement of 1 ppm or better, the beam properties must be held within tight constraints. In pursuit of this, the beam position must be measured to better than 25 μm per 33 ms time window and the beam current to 40 ppm during the same 33 ms time window. To accomplish this, $G\emptyset$ uses two sets of XYQ microwave cavity monitors. These monitors require precision electronics designed and built by TJNAF and TRIUMF. Specifically, the position monitors produce a voltage signal based on position for the X and Y cavities, and a current proportional voltage signal for the current cavity. The voltage is amplified by dedicated amplifiers designed specifically for the dynamic range of the cavities expected during the course of the $G\emptyset$ experiment. The output from these amplifiers is fed into TRIUMF-built precision voltage to frequency converters and thence into the $G\emptyset$ DAQ scalars.

One set of these XYQ cavities is installed approximately 30 m upstream of the $G\emptyset$ target. The second set of XYQ cavities is installed on the $G\emptyset$ diagnostic girder immediately before the target. Also on this girder are a pair of standard stripline beam position monitors, a pair of super-harp wire scanners, and an optical transmission view. The combination of these monitors will allow a beam position measurement of better than 10 μm per helicity window and an angle measurement of better than 0.5 μrad.

In addition to measuring and tightly controlling the beam properties, there will also be a need to determine the false asymmetries contributed by the beam parameters of position, angle, and current on target. Knowledge of the false-asymmetries is required in order to extract the physics asymmetries and its associated uncertainties. The false asymmetries are given by

$$\mathrm{A_f} = \sum \frac{\partial Y}{\partial X_i} \Delta X_i$$

where ∂Y is the change in the detector yield, ∂X_i is the change in the i^{th} beam parameter, and ΔX_i is the helicity correlated asymmetry per quartet. To calculate these false asymmetries, the sensitivities $\frac{\partial Y}{\partial X_i}$ must be measured. To accomplish this, deliberate and controlled beam modulation is introduced. This is accomplished by sending a dc current to beam steering magnets far upstream from the $G\emptyset$ target. The steering magnet positions are chosen to minimize $x - y$ motion coupling at the target. By modulating a specific beam parameter, $\{X,\ Y,\ \Theta_x,\ \Theta_y,\ E\ \}$, and noting the detector yield response, $\partial Y/\partial X_i$ can then be extracted. These slopes will be measured at the beginning of each data run while the helicity asymmetry will be measured continuously throughout the run. This modulation system has recently been tested with beam and works as expected. Shown in Figs. 27 and 28 are plots of the beam displacements resulting from modulation of the upstream steering coil.

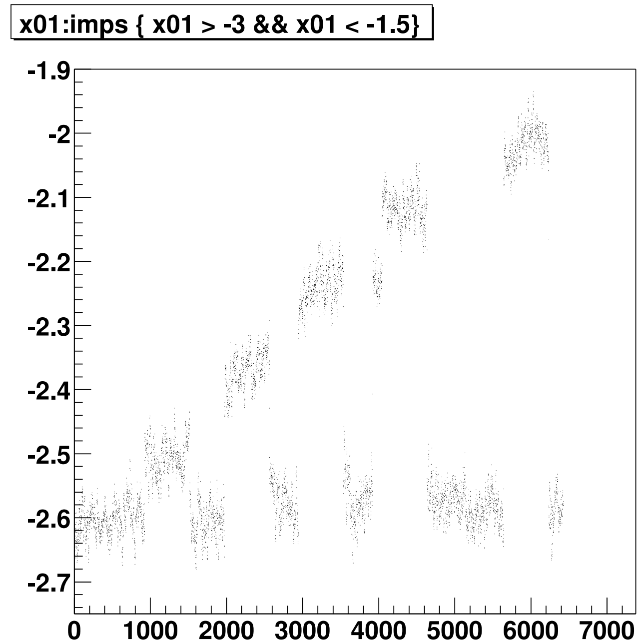

Fig. 27. Beam displacement resulting from modulation of upstream steering coils. The vertical axis gives a measure of the beam position (in mm) and the horizontal axis is in units of time (macro pulse signal).

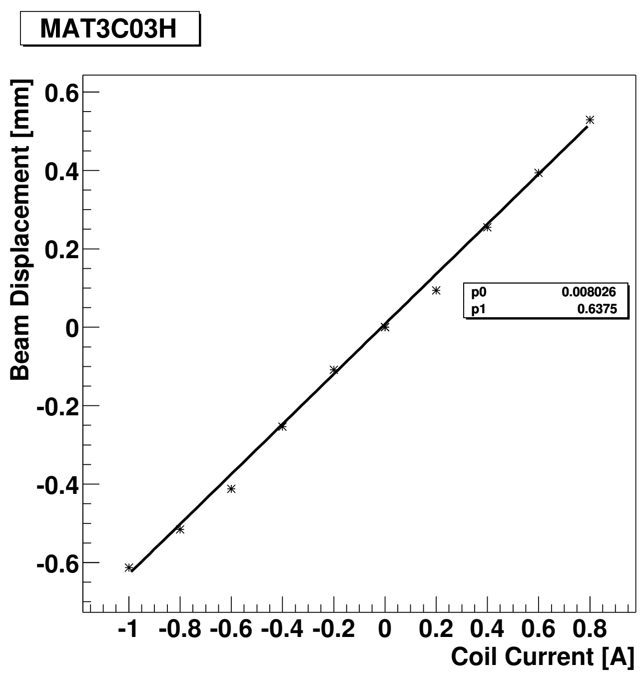

Fig. 28. Beam displacement as a function of steering coil excitation.

This modulation control system is being developed by members of the Canadian subgroup. Further developments of this system will include general beam/detector diagnostic software which will allow searches for the detector-magnet system asymmetry null coordinates, otherwise known as the sweet spot.

Target slow controls

The $G\emptyset$ experiment will use a 20 cm long liquid hydrogen (LH_2) target connected to a cryogenic loop to recirculate and cool the liquid. This target will operate at 20 K and 25 psia, and the heat deposited by the 40 μA electron beam will be carried away from the hydrogen by a compressed He gas heat exhanger. The main components of the target system are a pump for circulating the target fluid in a closed cryogenic loop, a heat exchanger, the target cell and a manifold to direct the fluid flow down the centre of the target cell. A gas handling system is employed to provide gas to the target, the He coolant to the heat exchanger, and to evacuate the region surrounding the target. The state of the target (temperatures, pressures, position, etc.) and the gas handling system (valve settings) is monitored/controlled by what is called the slow controls system. This system sounds alarms when operating conditions become improper, monitors beam current and maintains a constant heat load on the target. The controls system also includes recording the target state at regular intervals to log files. The Canadian subgroup has been providing design and implementation support for the liquid hydrogen target slow controls system. Specifically, the responsibilities include: (a) participation in MEDM monitoring and control screens design; (b) installation and integration into the system of the Joule-Thompson valve controller to control the flow of the He coolant; (c) testing of target and He coolant temperature sensors; (d) participation in the pressure transducer calibration and target motion testing/calibration; and (e) configuration and management of the channel archiver software which logs and plots the target data. Members of the Canadian subgroup have taken part in the test cooldowns of the target and are also involved in the design of the $G\emptyset$ main screen software which displays the experiment and system status.

Under typical experiment running conditions, the heavy data load will need to be managed and stored in an efficient way. These data will be decomposed into one of two types: physics data and slow control data. The physics data involves yields and asymmetries, whereas the slow control data consists of temperatures, pressures, vacuums of various subsystems (target, magnet) and beam parameters such as polarization or helicity. The University of Manitoba/TRIUMF group along with New Mexico State University (NMSU) is successfully carrying out the task of designing and implementing a MySQL database for the slow control part of the data. These data will be stored on a run by run basis and will be made available on the Web to the collaboration at large.

Engineering and commissioning runs

Several engineering runs have been carried out by the $G\emptyset$ collaboration, including studies of: (a) the helicity correlated properties of the TJNAF polarized electron beam and the noise characteristics of the Hall-C beam line monitors (July, 1997); and (b) the neutron background and energy spectrum in the vicinity of the $G\emptyset$ detector system (December, 1999). Both these efforts were coordinated by members of the Canadian subgroup and personnel from TJNAF (Hall-C) with much of the equipment provided by the Canadian subgroup.

This past year and a half, as the forward-angle mode of the $G\emptyset$ experiment entered the commissioning phase, the individually complex systems comprising the experiment had to be integrated into one overall system and tested. The commissioning was broken into three stages. The first stage, called the chain tests, was carried out from July through September, 2001. During this period, one fourth of the detector system was installed and cabled in the hall. In addition, about one half of the data acquisition system (DAQ), including the Trigger supervisor, was tested with beam in the hall. This test was used to identify shortcomings in the detector-DAQ-analysis chain. The second stage, carried out over the late summer and fall of 2002, involved the commissioning of the $G\emptyset$ cryogenic target, toroidal spectrometer and detector system with beam. The various subsystems were successfully commissioned, and the experiment is presently in the third stage, called the engineering run. The engineering run includes the fully operational spectrometer, the complete eight sector detection system, the full DAQ and electronics train, the cryogenic target system, $G\emptyset$ beam, beam modulation and beam diagnostics.

Canadian subgroup of the $G\emptyset$ collaboration: J. Birchall, J. Chang, B. Clemente, W.R. Falk, G. Faust, L. Lee, S.A. Page, W.D. Ramsay, A. Rauf, G. Rutledge, M. Steeds, W.T.H. van Oers (Manitoba); E. Korkmaz, T. Porcelli (Northern British Columbia); C.A. Davis (TRIUMF).

TJNAF Experiment 02-020

The Qweak experiment: a search for physics at the TeV scale via a measurement of the proton's weak charge

(S.A. Page, W.T.H. van Oers, Manitoba)

The standard model of electroweak interactions has been confirmed with impressive precision in a variety of experiments, ranging in energies from the eV scale in atomic parity violation to a few hundred GeV in collisions at HERA, LEP, SLC, and the Tevatron. Consequently, the particle physics community has turned from testing the standard model and measuring its parameters to searching for "new" physics beyond the standard model. In addition to searches for the Higgs boson, the searches for signatures of such new physics is one of the primary objectives of present and future high energy collider experiments.

However, an essential, but not well tested, prediction of the standard model is the variation of $\sin^2(\theta_W)$ with momentum transfer Q^2, referred to as the "running of $\sin^2(\theta_W)$" (see Fig. 29). Testing this prediction requires a set of precision measurements over a large range of Q^2 values, with sufficiently small and well understood theoretical uncertainties associated with the extraction of $\sin^2(\theta_W)$. It clearly requires a careful evaluation of the standard model radiative corrections to $\sin^2(\theta_W)$ in the context of the renormalization group evolution of the gauge couplings. This has been crucial in establishing QCD as the correct theory of the strong interaction. But the gauge coupling of the weak interaction, at low energies represented by the weak mixing angle $\sin^2(\theta_W)$, has not yet been studied successfully in this respect.

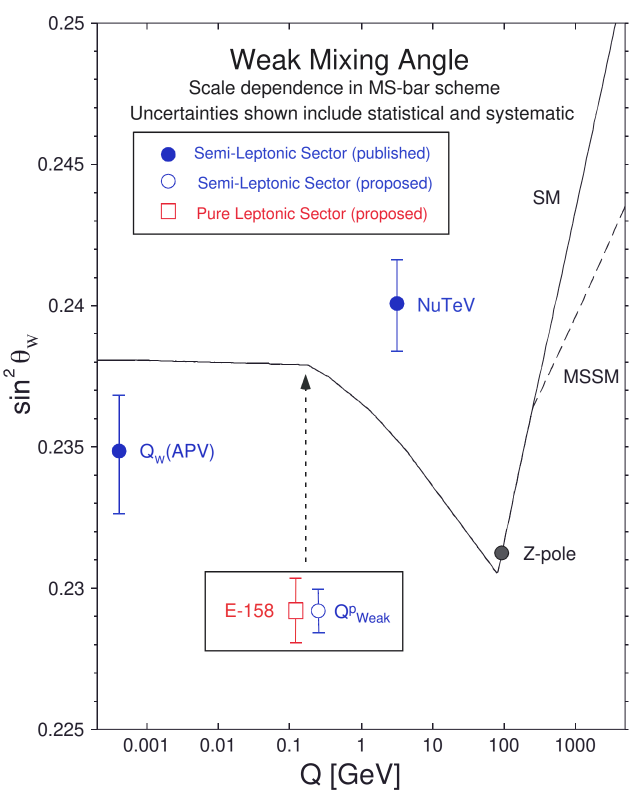

Fig. 29. Running of $\sin^2(\theta_W)$.

The standard model has a well defined prediction for the Q^2 dependence of $\sin^2(\theta_W)$. The very precise measurements at the Z^0 pole (at LEP and SLC) set the overall scale of the "running" of $\sin^2(\theta_W)$. Currently there are only two other measurements of $\sin^2(\theta_W)$ which test the running at a significant level: one from an atomic parity violation (APV) experiment (a 2.6 σ deviation below the predicted value) [Bennett and Wieman, Phys. Rev. Lett. **82**, 2484 (1999); Wood *et al.*, Science **275**, 1759 (1997)] and one from high energy neutrino-nucleus scattering [Zeller *et al.* (NuTeV collaboration), Phys. Rev. Lett. **88**, 091802 (2002)]. The proposed measurement of the weak charge of the proton will be performed with significantly smaller statistical and systematic errors and has a much cleaner theoretical interpretation than existing low Q^2 data. It is complementary to, and will be carried out to higher precision than an approved experiment at SLAC (E158) [SLAC Proposal E158, spokespersons E.W. Hughes, K. Kumar, and P.A. Souder], which will attempt to determine $\sin^2(\theta_W)$ from parity violating electron-electron (Moeller) scattering. The importance of a new measurement of the weak charge of the proton is underlined by the current situation in atomic parity violation. To date, the most precise measurement of low energy neutral current interactions has been carried out by exploiting parity violating effects in cesium, which allow a determination of the weak charge of the cesium nucleus. Unfortunately, there continue to be considerable theoretical atomic structure uncertainties. Very recently, the NuTeV collaboration determined $\sin^2(\theta_W)$ at a Q^2 value of about 10 (GeV/c)^2 in deep inelastic scattering of neutrinos in an iron/scintillator target. The result is about 3 σ above the predicted value. The uncertainty is claimed to be dominated by statistics. However, it is conceivable that isospin symmetry violating parton distribution functions are responsible for part of the effect. Both the measurement of the weak charge of the proton and the polarized Moeller scattering experiment E158 at SLAC should be able to measure the weak mixing angle at low energies to unprecedented precision. These experiments will have different systematic errors and complementary dependences on physics beyond the standard model [Kurylov *et al.*, hep-ph/0205183]. A 4% measurement of the weak charge of the proton corresponds to an uncertainty of ± 0.0007 in $\sin^2(\theta_W)$, and would establish the difference in radiative corrections between $\sin^2(\theta_W)$ at low Q^2 and $\sin^2(\theta_W)$ at the Z^0 pole as a 10 standard deviation effect. For comparison, the E158 experiment anticipates a combined statistical and systematic error of about 9% on the measured asymmetry.

The Qweak experiment will measure the parity violating asymmetry in polarized electron-proton scattering at very low momentum transfer (Q^2 value of 0.03 $(\mathrm{GeV/c})^2$) and an energy of 1.12 GeV. These experimental conditions will suppress the hadronic form factor contributions to the measured asymmetry. The results of earlier electron-proton parity violating experiments will be used to constrain these hadronic corrections to the data. A 2200 hour measurement of the parity violating asymmetry in electron-proton scattering at the momentum transfer of 0.03 $(\mathrm{GeV/c})^2$ employing 180 μA of 80% polarized beam on a 0.35 m liquid hydrogen target will determine the proton's weak charge with a 4% combined statistical and systematic error. A longitudinally polarized electron beam, a liquid hydrogen target, a resistive toroidal magnetic spectrometer, detectors for the scattered electrons at forward angles complete with electronics, and a dedicated Compton polarimeter are the key elements of the experimental apparatus. The toroidal magnetic field will focus elastically scattered electrons onto a set of eight, rectangular quartz Čerenkov detectors coupled to photomultiplier tubes, which will be read out in current mode to achieve the high statistical precision required for the measurements. The acceptance averaged asymmetry in the designed experiment is –0.3 ppm. The asymmetry will be measured to $\pm1.9\%$ statistical and $\pm1.7\%$ systematic error, leading to the determination of $\sin^2(\theta_W)$ at the 0.2% level.

Major stakeholders in the experiment are JLab, who will provide the polarized beam, the beam line instrumentation and required shielding, and the liquid hydrogen target; LANL, who lead the design and construction of the detector package and associated electronics; Louisiana Tech, who lead the effort in computer simulations of the detector and detector response; MIT-Bates, who will play a significant role in the design and implementation of a dedicated Compton polarimeter for the experiment; and the Manitoba/UNBC/TRIUMF group who are leading the magnetic spectrometer construction project.

The resistive toroidal magnet with eightfold symmetry has been defined in a working group meeting held at TRIUMF on July 22 in which physicists and engineers from JLab, Louisiana Tech, Manitoba, MIT-Bates, and TRIUMF participated. The engineering concept has been worked out in a series of follow-up meetings with MIT-Bates engineers at Jefferson Laboratory and TRIUMF. This has led to requests for quotes for the copper conductor wire, the eight coils, their support structure, and the power supply. These quotes are currently being evaluated. Simulations of the particle-tracking through magnetic field configurations deviating from the specified ideal field, as well as systematic error analyses, are under way.

Financial support has come from an NSERC International Opportunity Award and from discretionary funds at Jefferson Laboratory for the resistive toroidal magnet project, and from Los Alamos National Laboratory for development of the detector system. Research Instrumentation Grant and Project Grant applications for Qweak have been submitted to NSERC.

Canadian subgroup of the Qweak collaboration: J. Birchall, W.R. Falk, L. Lee, S.A. Page, W.D. Ramsay, G. Rutledge, W.T.H. van Oers, (Manitoba); E. Korkmaz, T. Porcelli, (Northern British Columbia); C.A. Davis, J. Doornbos, (TRIUMF).